Award Number: DAMD17-00-1-0081

TITLE: Targeting of Prostate Cancer with Hyaluronan
            Binding Proteins

PRINCIPAL INVESTIGATOR: Lurong Zhang, M.D., Ph.D.

CONTRACTING ORGANIZATION: Georgetown University
                           Washington, DC 20007

REPORT DATE: June 2003

TYPE OF REPORT: Annual

PREPARED FOR: U.S. Army Medical Research and Materiel Command
               Fort Detrick, Maryland 21702-5012

DISTRIBUTION STATEMENT: Approved for Public Release;
                        Distribution Unlimited

The views, opinions and/or findings contained in this report are
those of the author(s) and should not be construed as an official
Department of the Army position, policy or decision unless so
designated by other documentation.

20031104 080

REPORT DOCUMENTATION PAGE

Form Approved
OMB No. 074-0188

1. AGENCY USE ONLY (Leave blank)	2. REPORT DATE June 2003	3. REPORT TYPE AND DATES COVERED Annual (1 Jun 02 – 31 May 03)

4. TITLE AND SUBTITLE
Targeting of Prostate Cancer with Hyaluronan Binding Proteins

5. FUNDING NUMBERS
DAMD17-00-1-0081

6. AUTHOR(S)
Lurong Zhang, M.D., Ph.D.

7. PERFORMING ORGANIZATION NAME(S) AND ADDRESS(ES)
Georgetown University
Washington, DC 20007

E-Mail: zhangl@georgetown.edu

8. PERFORMING ORGANIZATION REPORT NUMBER

9. SPONSORING / MONITORING AGENCY NAME(S) AND ADDRESS(ES)
U.S. Army Medical Research and Materiel Command
Fort Detrick, Maryland 21702-5012

10. SPONSORING / MONITORING AGENCY REPORT NUMBER

11. SUPPLEMENTARY NOTES
Original contains color plates: All DTIC reproductions will be in black and white.

12a. DISTRIBUTION / AVAILABILITY STATEMENT
Approved for Public Release; Distribution Unlimited

12b. DISTRIBUTION CODE

13. ABSTRACT (Maximum 200 Words)

To test our hypothesis that the hyaluronan (HA) binding proteins (HABP) from cartilage is a new category of anti-tumor agents, we have proposed three aims: **1)** To examine the effect of HABP on the tumor growth of prostate cancer cell lines; **2)** To examine the effect of link protein and aggrecan on the tumor growth of prostate cancer; **3)** To examine the possible anti-angiogenesis effect of HABPs.

In past year, we have successfully finished the following works: **1)** cloned 1,065 bp of cDNA cording for full length of human cartilage link protein; **2)** inserted this cDNA into pcDNA3 expression vector; **3)** stably transfected into tumor cell lines; **4)** examined the inhibitory effect of link protein on growth of endothelial cells; **5)** demonstrated that the link protein could inhibit the tumor growth *in vivo*.

The significance of these studies are **1)** it determines that the link protein is an anti-tumor element in cartilage; **2)** the cDNA cloned in this study may be used for gene therapy.

14. SUBJECT TERMS
Hyaluronan-Binding Proteins, Experimental Therapy, Prostate Cancer, Angiogenesis

15. NUMBER OF PAGES
46

16. PRICE CODE

17. SECURITY CLASSIFICATION OF REPORT Unclassified	18. SECURITY CLASSIFICATION OF THIS PAGE Unclassified	19. SECURITY CLASSIFICATION OF ABSTRACT Unclassified	20. LIMITATION OF ABSTRACT Unlimited

NSN 7540-01-280-5500

Standard Form 298 (Rev. 2-89)
Prescribed by ANSI Std. Z39-18
298-102

Table of Contents

INTRODUCTION

While cancer is defined as an uncontrollable malignancy that highly dependent upon tumor angiogenesis (1), substances with anti-tumor/angiogenesis properties become very attractive to cancer patients (2-3).

Cartilage is an avascular tissue highly resistant to invasion by blood vessels when compared to other tissues (4). The fact that few tumors occur in cartilage may be related to this unique property.

For almost two decades, cartilage has been widely used by millions of cancer patients as an alternative medicine (5-13).

Although its anti-tumor effect is uncertain (12-14), and its mechanisms of action are largely unknown and its effective components have not as yet been well-defined (15), cartilage products still are the very popular alternative anti-cancer agents that widely accepted in USA, Canada, Europe and Eastern countries (such as China and Japan). This is largely due to the fact that in some patients, cartilage products do achieve anti-tumor/angiogenesis effects and extend patients' survival time.

However, it is unclear that which component in cartilage is responsible for its anti-tumor/angiogenesis effect. Since cartilage contains a large amount of hyaluronan (HA) and HA binding proteins (HABP), we speculate that HABP is responsible for the anti-tumor/angiogenesis effect of cartilage. This speculation is also based on the following observations: first, several proteins that bind to HA can also inhibit tumor growth or metastasis, such as soluble CD44 (16), RHAMM (17) and proteins from chondrocytes (18, 19); secondly, some angiogenic inhibitors, such as endostatin and angiostatin (20, 21), contain structural motifs that may allow them to bind to anionic proteoglycan (such as heparan sulphate and HA) and to interrupt the growth factor signaling (22).

In this project, we want to test our hypothesis that the hyaluronan (HA) binding proteins (HABP) from cartilage is a new category of anti-tumor agents. We have proposed to focus on three aims: 1) To examine the effect of HABP on the tumor growth of prostate cancer cell lines; 2) To examine the effect of link protein (LP) and aggrecan on the tumor growth of prostate cancer; 3) To examine the possible anti-angiogenesis effect of HABPs.

In **first year**, we demonstrated that the HABP purified from cartilage with affinity column have the following properties: 1) HABP can inhibit the anchorage-dependent and independent growth of tumor cells; 2) HABP can inhibit proliferation and migration of endothelial cells *in vitro* and angiogenesis *in vivo*; 3) HABP can reduce the growth of TSU prostate cancer and other tumor *in vivo*; 4) HABP can inhibit the experimental lung metastasis; 5) The anti-tumor effect of HABP is in part due to its anti-angiogenesis property. These results has been published in *Cancer Research* (2001; 61:1022-1028).

In **second year**, we have successfully cloned 993 bp of cDNA cording for N-terminus of human aggrecan, which consists of at least six HA binding motifs. We inserted the cDNA into yeast expression vector and purified the recombinant human aggrecan for the media of transformed yeast. We characterized that this recombinant aggrecan was highly glycosylated. Importantly, we demonstrated that the recombinant aggrecan could inhibit the proliferation of endothelial cells *in vitro* and demonstrated that the recombinant aggrecan could inhibit the tumor growth *in vivo*.

In the **past year**, we cloned 1,065 bp cDNA of human link protein, another component of HA binding protein from cartilage, and studied its anti-tumor effect. The results are summarized as following.

BODY

In our previous study (23), we have demonstrated that the HA binding proteins (HABPs) of cartilage possess anti-tumor/angiogenesis property.

There are at least two major HA binding proteins in cartilage as: aggrecan and the link protein. To dissect out which component is mainly responsible for the anti-tumor activity, we decide to use genetic engineering techniques to express each of these two components in the human form. If these human proteins turn out to be anti-tumor/angiogenesis, then, they may have the potential to be utilized for cancer therapy, since the proteins from human origin have little antigenicity and may not cause side-effect.

In last report, we demonstrated that the aggrecan of cartilage did exert anti-tumor/angiogenesis effect.

In the past year, we also used the genetic engineering approach to determine the anti-tumor activity of link protein (LP), another component of HABPs in cartilage.

1. Cloning, Construction and expression of human cartilage link protein (LP):

To obtain human cartilage LP, we had to use molecular biology approach, since it is impossible to directly obtain this human protein. According to the published cDNA sequence (GenBank access number X17405), the cartilage link protein has 354 amino acids (aa) with first 15 aa as a signal peptide for secretion. It has a theoretical pI of 7.10 and molecular weight of 40,166 Dalton.

MKSLLLLVLISICWADHLSDNYTLDHDRAIHIQAENGPHLLVEAEQAKVFSHRGGNVTLPCKFYRDP
TAFGSGIHKIRIKWTKLTSDYLKEVDVFVSMGYHKKTYGGYQGRVFLKGGSDSDASLVITDLTLED
YGRYKCEVIEGLEDDTVVVALDLQGVVFPYFPRLGRYNLNFHEAQQACLDQDAVIASFDQLYDAW
RGGLDWCNAGWLSDGSVQYPITKPREPCGGQNTVPGVRNYGFWDKDKSRYDVFCFTSNFNGRFY
YLIHPTKLTYDEAVQACLNDGAQIAKVGQIFAAWKILGYDRCDAGWLADGSVRYPISRPRRRCSPT
EAAVRFVGFPDKKHKLYGVYCFRAYN

Based on this sequence, to clone the cDNA cording for LP we designed a pair of primers that framed from ATG start cordon to TGA stop cordon with EcoR I site at 5'-end and Xho I site on 3'-end, respectively. The RT-PCR was performed using a cDNA library of a human sarcoma cell line derived from chondrocytes as a template. A RT-PCR product with a length of 1,065 bp was obtained (**Fig. 1A**).

The cDNA cording for link protein was cut with EcoR I and Xho I, and then inserted into pcDNA3 mammalian expression vector (Invitrogen, Inc, **Fig. 1B**). When DNA sequence was performed, the result indicated that there was no error in RT-PCR and reading frame.
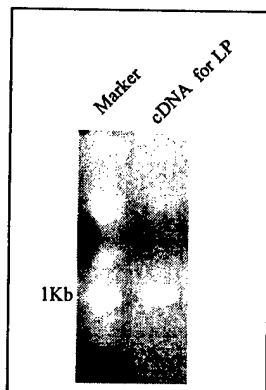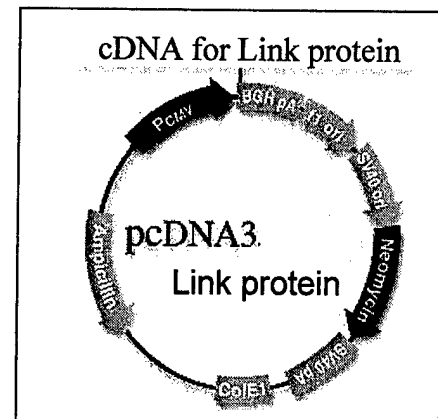

Fig. 1: Cloning and Construction of human cartilage link protein. A: RT-PCR product of human cartilage link protein Lane 1: Marker; Lane 2: A correct RT-PCR product with a length of 1,065 bp; **B:** pcDNA3-link protein expression vector.

With the assurance of correct DNA sequencing, the link protein expression vector was transfected into TSU tumor cells (recently TSU has been regarded as a bladder cancer cell line instead of prostate cancer cells) and MDA231 tumor cells to determine whether the anti-tumor effect, if any, is not tumor cells specific and possesses a common anti-tumor effect applicable to multiple types of tumors.

The stable gene transfection was conducted with calcium precipitation method. The pcDNA3 vector alone was also transfected as mock control. The cells survived in 800 µg/ml of G418 were picked up, expanded and then pooled for further study to avoid the clonal variation.

To detect the expression of link protein in transfected cells, dot blot was performed using anti-link protein monoclonal antibody. Equal amount supernatant (1 ml) from the same density of pcDNA3 vector alone control transfactants or pcDNA3-LP transfectants was analyzed. The results (**Fig. 2**) indicated that the level of link protein (LP) in the supernatant of transfected tumor cells was much higher than that in mock controls, indicating that the transfected cells indeed expressed a high level of human cartilage link as compared to parental tumor cells.
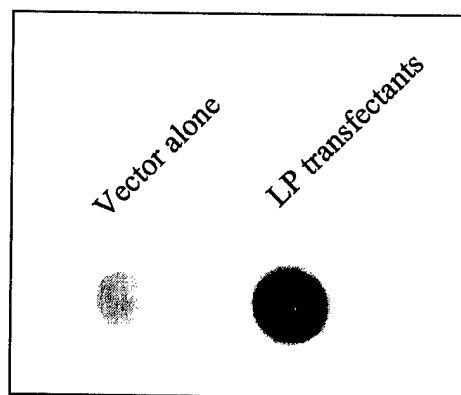

Fig. 2. The expression of link protein in transfected cells: One ml of supernatant of transfected tumor cells was mixed with 70 µl of HA-Sepharose 4 B and shaken overnight. Next day, the beads were washed with 0.05% PBS-Tween 20 for times to discarded the miscellaneous proteins and the bounded link protein were eluted with 40 µl of loading buffer and boiling for 5 min. The samples were loaded on nitrocellulose membrane and stained with anti-human cartilage link protein. The mock transfectants did not express link protein (**A**), while there is abundant link protein in the pcDNA3-LP transfectants (**B**).

2. Effect of link protein on endothelial cells

It has been proved that avascular cartilage contains anti-angiogenesis agents, which is responsible for its anti-tumor activity (23). To see if this is possessed by link protein, the conditional media obtained from pcDNA3-LP transfectants was added to equal amount of bovine capillary endothelial cells (BCE) and the effect on their growth was determined by counting of cell numbers at different groups.

The result (**Fig. 3**) indicated that the LP had an inhibitory effect on the proliferation of endothelial cells. The difference between the test and the control was statistically significant (p<0.05).
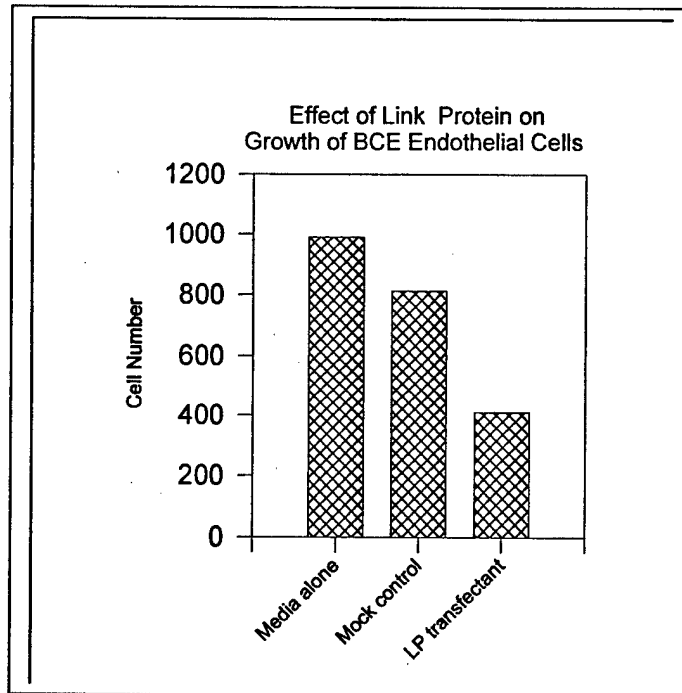
Fig. 3. Effect of link protein on endothelial cells. The conditional medial from transfectants was added to media of bovine capillary endothelial cells (BCE) cultured in 24 well plate for two days. The BCE cells were harvested with 10 mM EDTA-PBS and counted with Coulter counter. There was a difference between the LP group and control groups (p<0.05).

3. In vivo anti-tumor effect of human cartilage link protein

We then examined if human cartilage link protein has any effect on tumor growth. Two million of pcDNA3-LP transfectants or pcDNA3 vector alone transfectants were subcutaneously injected into 5 week old nude mice (5 mice /group). The tumor sizes were measured twice per week and the tumor volume was calculated. Four-weeks later, the tumor bearing mice were pictured, and the tumors were harvested and weighted. The results showed that the tumors formed by pcDNA3-LP transfectants were much smaller than those formed by pcDNA3 vector alone transfectants (**Fig. 4A**) and the difference in the tumor weight (**Fig. 4B**) and tumor volume (**Fig. 4C**) between two groups was statistically significant (P<0.05). There was no difference in the body weight between two groups, indicating that there was not side effect with this anti-tumor approach.
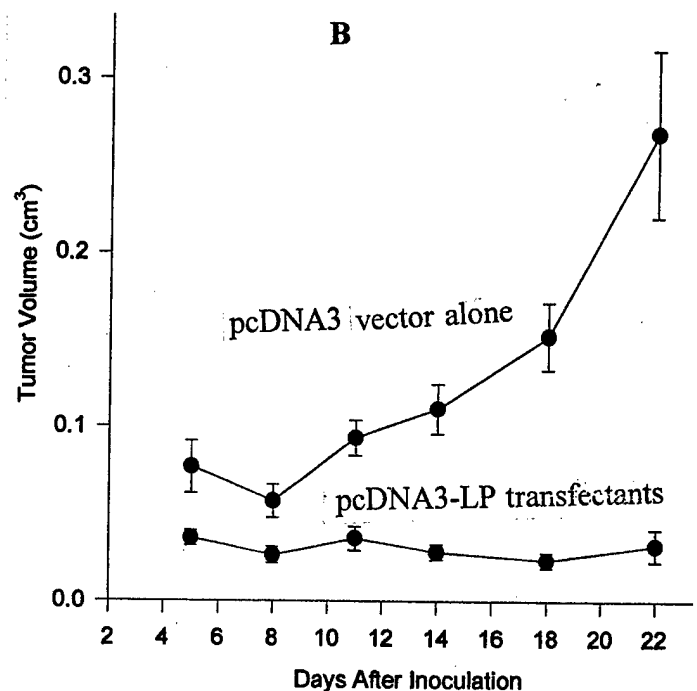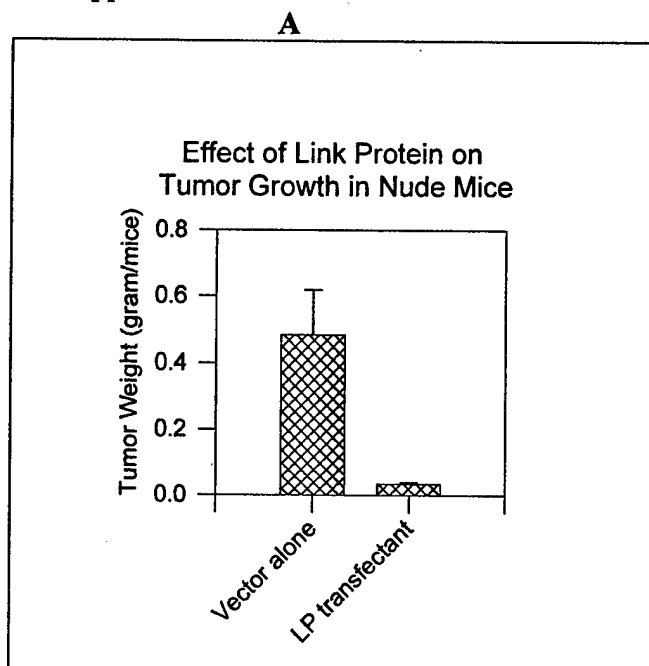
Tumor growth of mock transfectants

Tumor growth of pcDNA3-link protein transfectants

Fig 4. *In vivo* anti-tumor effect of link protein. . Two million of pcDNA3-LP transfectants or pcDNA3 vector alone transfectants were subcutaneously injected into 5 week old nude mice (5 mice /group). The tumor sizes were measured twice per week and the tumor volume was calculated. Four-weeks later, the tumor bearing mice were pictured, and the tumors were harvested and weighted. **A:** Tumor weights; **B:** Tumor growth curve; and **C:** Pictures of tumor size. Compared to the control, the link protein strongly inhibited the tumor growth *in vivo* (P<0.05).

4. Attempt to obtain recombinant human cartilage link protein

When the in vivo results demonstrated that the human cartilage link protein possessed anti-tumor effect, we started to make effort on obtaining recombinant human cartilage link protein using yeast expression and affinity purification approaches, based on the rationale that the recombinant human cartilage link protein may be practical for clinical use. We have successfully constructed the pPICZ-LP yeast expression vector that contained with α-factor signal peptide for secretion of LP from yeast cells and His$_6$ tag for purification. However, we failed in obtaining the sufficient amount of recombinant human link protein to do any experiments *in vitro* or *in vivo*. We tried very hard to figure out the problems by two postdoctoral follows. The conclusion was that for some unknown reasons, the link protein was expressed at a low level in two different yeast systems and hard to obtain sufficient amount by Ni-affinity column. We need to reconsider our strategy and find a new system to do this.

In summary, in past year, we have successfully finished the following works: **1)** cloned 1,065 bp of cDNA cording for full length of human cartilage link protein; **2)** inserted this cDNA into pcDNA3 expression vector; **3)** stablely transfected into tumor cell lines; **4)** examined the inhibitory effect of link protein on growth of endothelial cells; **5)** demonstrated that the link protein could inhibit the tumor growth *in vivo*.

The significance of these studies are **1)** it determines that the link protein is an anti-tumor element in cartilage; **2)** the cDNA cloned in this study may be used for gene therapy.

Since the underlying mechanisms by which the components of avascular cartilage exert their anti-tumor effect are largely unknown, we will focus on the mechanism study using the material or cell lines obtained, if possible, we will further dissect out the functional motifs of these anti-tumor proteins from HA binding proteins.

We believe the study will help in solving the puzzles: what is the molecular basis of widely used cartilage in the battle of anti-cancer and how we can better utilize the research result to make the anti-tumor elements of cartilage become more powerful in treatment of prostate cancer.

Key Research Accomplishments

Taken together, **in past year,** we have successfully finished the following works: **1)** cloned 1,065 bp of cDNA cording for full length of human cartilage link protein; **2)** inserted this cDNA into pcDNA3 expression vector; **3)** stably transfected into tumor cell lines; **4)** examined the inhibitory effect of link protein on growth of endothelial cells; **5)** demonstrated that the link protein could inhibit the tumor growth *in vivo*.

The significance of these studies are **1)** it determines that the link protein is an anti-tumor element in cartilage; **2)** the cDNA cloned in this study may be used for gene therapy.

Conclusions

- The link protein from human cartilage can be expressed in tumor cells.

- The link protein in conditional media can inhibit the growth of endothelial cells *in vitro*.

- The link protein can inhibit the tumor cell growth in nude mice model system.

- The cDNA cloned in this study may be used for gene therapy.

Reportable outcomes

(Due to or partially due to this support)

Papers

1. Shanmin Yang, Jinguo Chen, Zhen Guo , Xue-Ming Xu, Luping Wang, Xu-Fang Pei, Jing Yang' Charles B. Underhill and Lurong Zhang' Triptolide Inhibits the Growth and Metastasis of Solid Tumors. Mol Cancer Ther. 2003; 2(1):65-72.

2. Luping Wang, Jiyao Yu, Jian Ni, Xue-Ming Xu, Jianjin Wang, Haoyong Ning, Xu-Fang Pei, Jinguo Chen, Shanmin Yang, Charles B. Underhill, Lei Liu, Joeri Liekens, Joseph Merregaert and Lurong Zhang: Extracellular Matrix Protein1 (ECM1) is Over-expressed In Malignant Epithelial Tumors. Cancer Letter 2003; in press

3. Xue-Ming Xu, Yixin Chen, Feng Gao, Jinguo Chen, Shanmin Yang, Charles B. Underhill and Lurong Zhang: A Peptide with Three Hyaluronan Binding Motifs Inhibits Tumor Growth by Inducing Apoptosis. Cancer Res. 2003; revised

Abstracts

1. Jinguo Chen, Glenn D. Prestwich, Yi Luo, Xueming Xu, Shanmin Yang, Luping Wang, Charles B. Underhill and Lurong Zhang.: Inhibition of tumor growth and metastasis by hyaluronan conjugated Taxol. Proc. Annu. Meet. Am. Assoc. Cancer Res 2003; 44:1654

2. Luping Wang, Sunghee Kim, Jinguo Chen, Xue-Ming Xu, Shanmin Yang, Charles B. Underhill, and Lurong Zhang: Decoy TR6 protects tumor cells from apoptosis. Proc. Annu. Meet. Am. Assoc. Cancer Res 2003; 44: 149

3. Xue-Ming Xu, Ningfei Liu, Jinguo Chen, Luping Wang, Shanmin Yang, Charles B. Underhill, and Lurong Zhang. A Hyaluronan Binding Peptide can Trigger Apoptosis by Antagonizing Members of the Bcl-2 Family. Proc. Annu. Meet. Am. Assoc. Cancer Res 2003; 44: 5589

4. Shanmin Yang, Jinguo Chen, Xue-Ming Xu, Luping Wang, Charles B. Underhill and Lurong Zhang. Liposomal Triptolide inhibits tumor growth at a low dose. Proc. Annu. Meet. Am. Assoc. Cancer Res 2003; 44: 6461

References

1. Marwick C.: Natural compounds show antiangiogenic activity. J Natl Cancer Inst 2001; 93(22): 1685
2. Miller DR, et al: Phase I/II trial of the safety and efficacy of shark cartilage in the treatment of advanced cancer. J Clin Oncol. 1998; 16(11):3649-55
3. Couzin J.: Beefed-up NIH center probes unconventional therapies. Science. 1998;282(5397):2175-6
4. Lee A, et al: Shark cartilage contains inhibitors of tumor angiogenesis. Science. 1983; 221 (4616):1185-7.
5. Oikawa T, et al: A novel angiogenic inhibitor derived from Japanese shark cartilage (I). Extraction and estimation of inhibitory activities toward tumor and embryonic angiogenesis.Cancer Lett. 1990;51(3):181-6.
6. Horsman MR, et al: The effect of shark cartilage extracts on the growth and metastatic spread of the SCCVII carcinoma. Acta Oncol. 1998; 37(5): 441-5.
7. Simone CB, et al: Shark cartilage for cancer. Lancet. 1998; 9; 351(9113): 1440.
8. Newman V, et al: Dietary supplement use by women at risk for breast cancer recurrence. The Women's Healthy Eating and Living Study Group. J Am Diet Assoc. 1998; 98(3): 285-92.
9. Markman M: Shark cartilage: the Laetrile of the 1990s. Cleve Clin J Med. 1996; 63(3): 179-80.
10. Hunt TJ, et al: Shark cartilage for cancer treatment. Am J Health Syst Pharm. 1995; 52(16): 1756, 1760.
11. Mathews J: Media feeds frenzy over shark cartilage as cancer treatment. J Natl Cancer Inst. 1993; 4; 85(15): 1190-1.
12. Blackadar CB: Skeptics of oral administration of shark cartilage. J Natl Cancer Inst. 1993; 85(23): 1961-2.
13. Ernst E: Shark cartilage for cancer? Lancet. 1998; 24; 351(9098): 298.
14. Horsman MR, Alsner J, Overgaard J.: The effect of shark cartilage extracts on the growth and metastatic spread of the SCCVII carcinoma. Acta Oncol 1998; 37(5):441-5
15. Gonzalez RP, Leyva A, Moraes MO.: Shark cartilage as source of antiangiogenic compounds: from basic to clinical research. Biol Pharm Bull 2001; 24(10):1097-101
16. Sy, M-S., Guo, Y. J., and Stamenkovic, I.: Inhibition of tumor growth in vivo with a soluble CD44-immunoglobulin fusion protein. J. Exp. Med. 1992; 176: 623-627
17. Mohapatra S, Yang X, Wright JA, Turley EA, Greenberg AH: Soluble hyaluronan receptor RHAMM induces mitotic arrest by suppressing Cdc2 and cyclin B1 expression. J Exp Med 1996;183(4):1663-8
18. Moses, M A, Sudhalter, J., and Langer, R.: Identification of an inhibitor of neovascularization from cartilage. Science 1990; 248: 1408-1410
19. Moses, M A, Sudhalter, J., and Langer, R.: Isolation and characterization of an inhibitor of neovascularization from scapular chondrocytes. J. Cell Biol. 1992: 119 (2):473-482
20. O'Reilly MS. Boehm T. Shing Y. Fukai N. Vasios G. Lane WS. Flynn E. Birkhead JR. Olsen BR. Folkman J.: Endostatin: an endogenous inhibitor of angiogenesis and tumor growth. Cell 1997; 88(2):277-85
21. O'Reilly MS, Holmgren L, Shing Y, Chen C, Rosenthal RA, Moses M, Lane WS, Cao Y, Sage EH, Folkman J: Angiostatin: a novel angiogenesis inhibitor that mediates the suppression of metastases by a Lewis lung carcinoma. Cell 1994;79(2):315-28
22. Hohenester E. Sasaki T. Olsen BR. Timpl R.: Crystal structure of the angiogenesis inhibitor endostatin at 1.5 A resolution. EMBO Journal 1998; 17(6):1656-64
23. Ningfei Liu, Charles B. Underhill, Randall Lapevich , Zeqiu Han, Feng Gao, Lurong Zhang and Shawn Green: Metastatin: A hyaluronan binding complex from cartilage that inhibits tumor growth. Cancer Res 2001; 61:1022-1028

#149   Decoy TR6 protects tumor cells from apoptosis. Luping Wang, Sung-hee Kim, Jinguo Chen, Xue-Ming Xu, Shanmin Yang, Charles B. Underhill, and Lurong Zhang. *Beijing General Hospital, Beijing, China, Human Genome Sciences, Inc., Rockville, MD, Lombardi Cancer Center, Washington, DC, Xiamen University, Xiamen, China, and Fujian Medical University, Fuzhou, China.*

Recently, TR6, a decoy receptor of the TNFR super-family, has been shown to bind to three ligands: FasL, LIGHT and TL1. Since TR6 lacks a transmembrane domain, it can bind to these ligands and competitively block their interaction with Fas and HVEM and as a consequence inhibit apoptosis. In a series of experiments, we examined the role of TR6 in tumor progression, and obtained the following results: 1) in transwell chambers, the TR6 expressed by SW480 cells in the top well could inhibit apoptosis in MDA-435 tumor cells growing in the bottom well; 2) recombinant TR6 could block apoptosis induced by exogenous FasL and this effect could be reversed by the addition of neutralizing antibodies to TR6; and 3) cell death induced by endogenous FasL could be blocked by the addition of TR6. We then examined the expression of TR6 in a panel of human tissues by immunohis-tochemical staining with a monoclonal antibody and found that while normal tissue demonstrated little or no staining, a significant fraction of breast cancer tissue was positive. This fraction depended in part on the stage of the tumor. In the case of tumors that had not metastasized to the lymph nodes, the staining rate was 44% (4 out of 9) and for tumors that had metastasized the rate was 70% (14 out of 20). For lymph node metastases themselves, the rate was 80% (16 out of 20). Furthermore, ELISA assays showed that the level of TR6 in the serum of cancer patients was higher than that from normal individuals (2.3 + 0.2 ng/ml vs. 0.46 + 0.07 ng/ml). These results suggest that TR6 plays a critical role in preventing tumor cells from undergoing apoptosis and thereby promotes their progression. Thus, it may be possible to reduce tumor malignancy by inhibiting the function of TR6.

#5589   A hyaluronan binding peptide can trigger apoptosis by antagonizing members of the bcl-2 family. Xueming Xu, Ningfei Liu, Jinguo Chen, Luping Wang, Shanmin Yang, Charles B. Underhill, and Lurong Zhang. *Georgetown University Medical Center, Washington, DC, Shanghai 9th Hospital, Shanghai, China, Lombardi Cancer Center, Washington, DC, Beijing General Hospital, Beijing, China, and Xiamen University, Xiamen, China.*

In previous studies, we have demonstrated that the growth of tumor cells can be suppressed by a peptide termed P4 that can bind to hyaluronan. This effect appeared to be due to the induction of apoptosis, since treatment of cultured cells with P4 resulted in the fragmentation of the DNA, characteristic apoptotic cells. Confocal microscopy of cells treated with FITC tagged P4, revealed that it quickly became associated with mitochondria. This was further supported by the fact that treatment of cells with P4 induced a spectral change in the dye JC-1 indicating the loss of membrane potential in the mitochondria. Western blotting of cultured MDA-435 tumor cells following treatment with P4 revealed increased levels of activated caspase 9, caspase 3 and PARP, suggesting that P4 upregulated a Fas-independent pathway leading to apoptosis. Using immunoprecipitation, we found that the P4 peptide could bind to Bcl-2 and Bcl-xL which are predominately located in the membranes of mitochondria. And finally, in an in vitro assay with cytoplasmic extracts of tumor cells, we found that P4 caused the release of cytochrome c from the mitochondria. Taken together, these results suggest that P4 targets mitochondria by binding to Bcl-2 family members and this induces the release of cytochrome c leading to apoptosis.

#6461 Liposomal Triptolide inhibits tumor growth at a low dose. Shanmin Yang, Jinguo Chen, Xue-Ming Xu, Luping Wang, Charles B. Underhill, and Lurong Zhang. *Xiamen University, Xiamen, China, Lombardi Cancer Center, Washington, DC, Beijing General Hospital, Beijing, China, and Fujian Medical University, Fuzhou, China.*

Triptolide (TPL) is a compound purified from the herb Tripterygium wilfordii Hook F, and is highly effective against tumor growth, but has a low therapeutic window (i.e. concentrations having therapeutic effects are close to those having toxic effects). In an effort to improve it therapeutic window, we examined a formulation in which the TPL was incorporated into polyethylene glycol coated liposomes (PEG-Lipo-TPL). When tested on MDA-435 tumor cells growing in tissue culture, the effects of PEG-Lipo-TPL and TPL alone depended upon the time course. During the first six hours of exposure, PEG-Lipo-TPL induced only a 10% inhibition of thymidine incorporation while TPL alone induced a 50% inhibition rate. This difference may be due to the fact that free TPL could readily enter the tumor cells while PEG-Lipo-TPL needed more time to gain access to the cells. However, at 12 and 48 hours, both forms had a similar effect on the thymidine incorporation. We then tested both PEG-Lipo-TPL and TPL alone for their therapeutic windows in C57BL/6 mice. In both formulations, the TD50 (50% of toxic dose) was determined to be 1.3 mg/kg. However, the effective dose against the growth of B16 tumor xenografts was lower for the PEG-Lipo-TPL formulation than for TPL alone (0.25 mg/kg vs. 0.40 mg/kg). These results suggested that the liposomal formulation of TPL may indeed increase its therapeutic window, however more experiments are need to confirm this conclusion.

#1654 Inhibition of tumor growth and metastasis by hyaluronan conjugated taxol. Jinguo Chen, Glenn D. Prestwich, Yi Luo, Xueming Xu, Shanmin Yang, Luping Wang, Charles B. Underhill, and Lurong Zhang. *Lombardi Cancer Center, Georgetown University, Washington, DC and The University of Utah, Salt Lake City, UT.*

Previously, we have demonstrated that hyaluronan (HA) conjugated taxol (HA-taxol) shows selective toxicity to several human cancer cells growing in tissue culture. In this study, we examined the anti-tumor effects of HA-taxol on tumor xenografts growing in mice. As targets, we used human TSU bladder cancer cells and mouse 4T1 breast cancer cells, both of which express the HA receptor CD44 and were able to bind, internalize and degrade the HA. The growth of these cells as xenografts in mice was inhibited to a greater extent by the i.v. injection of HA-taxol than by taxol alone. To examine the turn-over of HA, we i.v. injected 3H-HA into mice and then examined its distribution. We found that in addition to the tumors, much of the 3H-HA was taken up by the liver and kidneys. However, if we injected chondroitin sulfate (CS) into the mice 2 hours prior to the administration of 3H-HA then this reduced the uptake of 3H-HA by the liver and increase the amount of 3H-HA that accumulated in the tumor xenografts. When mice with tumor xenografts were treated with CS and then HA-taxol, their survival time was longer than those treated with vehicle or HA-taxol alone. Furthermore, HA-taxol reduced the size of 4T1 cell metastases in popliteal and inguinal lymph nodes (35% and 64% respectively) to a greater extent than taxol alone (-1.7% and 31.8% respectively). Taken together, these results suggest that HA-taxol is more effective in treatment of metastasis than taxol alone and that the sequential use of CS and HA-taxol improves the targeting of tumors.

Extracellular Matrix Protein 1 (ECM1) is Over-Expressed In Malignant Epithelial Tumors

Luping Wang[1, 2], Jiyao Yu[3], Jian Ni[4], Xue-Ming Xu[1], Jianjin Wang[5], Haoyong Ning[4], Xu-Fang Pei[1], Jinguo Chen[1], Shanmin Yang[1, 6], Charles B. Underhill[1], Lei Liu[7], Joeri Liekens[8], Joseph Merregaert[8] and Lurong Zhang[1, 6]

[1]Department of Oncology, Lombardi Cancer Center, Georgetown University, 3970 Reservoir Road, NW, Washington DC 20007, [2]Dept. of Pathology, Beijing General Hospital, Beijing, P.R. China; [3]Dept. of Pathology, Naval General Hospital, Beijing, P.R. China; [4]Human Genome Sciences, Inc., 9410 Key West Avenue, Rockville, MD 20850; [5]Dept. of Pathology, Changhai Hospital, Shanghai, P.R. China; [6]The Key Laboratory of China Education Ministry on Cell Biology and Tumor cell Engineering, Xiamen University, Fujian, P.R. China; [7]Cybrdi Inc. Rockville, MD20850; [8]Laboratory of Molecular Biotechnology, Department Biomedical Sciences, University of Antwerp, Universiteitsplein1, B-2610 Wilrijk, Belgium

Lurong Zhang and Jozef Merregaert share senior authorship.

Corresponding author: Lurong Zhang, Department of Oncology, Lombardi Cancer Center, Georgetown University, 3970 Reservoir Road, NW, Washington DC 20007; Tel: 202-687-6397; FAX: 202-687-7505; E-mail: zhangl@georgetown.edu

Running title: Expression of ECM1 in tumors

ABSTRACT

The extracellular matrix protein 1 (ECM1) is a secreted protein that has been implicated with cell proliferation, angiogenesis and differentiation. In the present study, we used immunohistochemical staining to examine the expression of ECM1 in a panel of human tumors and found that it was closely correlated with some types of tumors including: invasive breast ductal carcinoma (83%), esophageal squamous carcinoma (73%), gastric cancer (88%) and colorectal cancer (78%). Significantly, ECM1expression was correlated with the metastatic properties of the tumors. Primary breast cancers that had formed metastases were 76% positive while those that had not metastasized were only 33% positive. ECM1 expression was also correlated with PCNA a marker for proliferation, but not with CD34, a marker for endothelial cells. These results indicate that ECM1 tends to be preferentially expressed by metastatic epithelial tumors.

Key words: ECM1, Proliferation, Metastasis, Endothelial Cells

1. Introduction

The extracellular matrix protein 1 (ECM1) was originally identified as an 85 kDa glycoprotein secreted by a murine osteogenic stromal cell line [1]. Subsequently, two forms of human ECM1 were described: ECM1a (68 kDa) which is the full length form consisting of 540 amino acids; and ECM1b (46 kDa) which is an alternatively spliced form with 415 amino acids [3]. These two forms of ECM1 are coded by a single gene, which has been mapped to 1q21 outside of the epidermal differentiation complex region [3, 4].

The distribution of ECM1 changes as a function of embryonic development. In mouse embryos, ECM1a is present in a number of tissues and is particularly prominent in blood vessels [2, 3, 5, 6]. Indeed, its expression pattern is similar to that of flk-1, a recognized marker for endothelial cells [6]. As development progresses, ECM1b is expressed in the tail, front paws and skin [3]. In adult humans, ECM1a is predominantly expressed by the skin [5], tonsils, heart and placenta [3]. In the case of the skin, ECM1a is restricted to the basal cell layer, while ECM1b is predominantly found in the suprabasal layers [3, 5].

Recent studies have implicated ECM1 with a number of physiological functions. For example, ECM1 appears to help regulate endochondral bone formation. Merregaert and his coworkers found that Ecm1 is expressed in the connective tissues surrounding the developing bones (perichondrium), but not in cartilage itself. At low concentrations, recombinant ECM1 stimulated alkaline phosphatase activity, whereas at higher concentrations, it inhibited alkaline phosphatase activity and mineralization [7]. In addition, ECM1 may be involved in the differentiation of keratinocytes as suggested by the fact that it is expressed in the skin and its gene is located is located close to the epidermal differentiation complex at 1q21 [3, 5]. Recently, Hamada and co-workers identified a homozygous loss-of-function mutation in the ECM1 gene in a family suffering from lipoid proteinosis, a rare, autosomal recessive disorder also called Urbach-Wiete disease [8-14]. The loss of functional ECM1 appears to be responsible for the classical

symptoms of which include thickening of the skin, mucosa and certain viscera the widespread deposition of hyaline (glycoprotein) and disruption of the basement membrane [8-14]. The secretion of ECM1 appears to be required for the maintenance of the extracellular matrix in the skin and mucosa.

In a recent study, we had found that ECM1 may also promote both cell proliferation and angiogenesis [6]. When a highly purified preparation of ECM1 was added to cultures of HUVEC, ABAE, BREC and BCE cells in serum-free medium, their growth was significantly stimulated as measured by thymidine incorporation. Under these conditions, the stimulation induced by ECM1 was only slightly less than that of FGF-2 and VEGF. However, the stimulatory effects of ECM1 appeared to be cell line specific in that MDA-435, MDA-468 and TSU cells showed little or no response. In another set of experiments, we found that ECM1 can also promote angiogenesis. A highly purified preparation of ECM1 was applied to small pieces of filter paper that were then applied to the chorioallantoic membranes of chicken eggs and two days later this region was subjected to computerized image analysis. The results of this analysis indicated that ECM1 had a marked stimulatory effect on degree of vascularization. Given the fact that ECM1 has been implicated with cell proliferation and angiogenesis, it also seemed possible that ECM1 may also contribute to tumor progression. Indeed, in this same study we had found that ECM1 could be detected in some breast cancer tissues, including metastases to both the lymph node and bone [6].

In the present study we have examined the expression of ECM1 in a panel of human tumors with affinity-purified antibodies against ECM1. Our goal here was two fold: first to determine if ECM1 expression could be used as a marker for a particular pathological condition; and secondly to test whether it was correlated with markers of tumor proliferation and angiogenesis. The results of this study indicated that several types of human epithelial malignant tumors expressed significant levels of ECM1 and that its expression was indeed correlated with tumor proliferation but not with angiogenesis.

4

2. Materials and methods

2.1. Patients and tissues samples

Both paraffin-embedded (296 sections from 263 cases) and fresh-frozen (10 cases) samples of human tumors were obtained from the tumor bank of Lombardi Cancer Center at Georgetown University, Pathology Departments of Beijing General Hospital and Naval General Hospital in Beijing, Changhai Hospital in Shanghai, and tissue array samples from Cybrdi (Rockville, MD). For the paraffin-embedded samples, 5 μm thick sections were stained with hematoxylin and eosin and then evaluated according to the W.H.O histopathological classification criteria. For the frozen tissues, OCT embedded blocks were cut into 7 μm thick sections and stained with hematoxylin and eosin for the pathological diagnosis, while the remainder of the tissue was homogenized in lysis buffer for Western blotting (see below). Frozen sections were also used for double label staining of both ECM1 and CD34 to preserve antigenicity. Among the tissues examined, there were a number of paired samples of both primary and metastatic tumors from the same patient, including 13 pairs from patients with breast cancer and 20 pairs from patients with lung cancer. Nine cases of breast cancer and 10 cases of lung cancer without metastasis were used for comparison.

2.2. Preparation of ECM1 Antibodies

Antiserum against human ECM1 was raised by injecting 0.2 mg of highly purified recombinant ECM1a or ECM1b in Freund's complete adjuvant (Difco, Sparks, MD) subcutaneously into rabbits. A second injection was given three weeks later and subsequent boosts were repeated every three weeks. The rabbit anti-ECM1 serum was collected every third week and the titer was determined by an ELISA. The antiserum generated by immunization with ECM1a cross-reacted with ECM1b and vice versa, since the sequence of ECM1b is identical to that of ECM1a with the exception of 125 amino acids missing from the central portion. The antibodies were further purified by affinity chromatography on ECM1 coupled to

5

Sepharose 4B. As described previously, the specificity of the ECM1 antibody was demonstrated by the fact that on Western blots of tissue extracts, it stained ECM1a and ECM1b as a single bands with little or no cross-reaction to any other protein [6].

2.3. Immunohistochemic staining

Paraffin sections were de-paraffined, dehydrated and incubated in a 10% hydrogen peroxide solution for 10 min to eliminate endogenous peroxidase activity. After thorough washing, the sections were incubated with affinity purified rabbit anti-ECM1 antibody (1:400) followed by anti-rabbit ABC staining procedure (Biostain Super ABC Kits, Biomeda) and the peroxidase substrate 3-amino-9-ethyl-carbazole (AEC) and H_2O_2, which gives a red reaction product. The samples were then counter-stained with hematoxylin (blue) and preserved with CrystalMount (Biomeda, Foster City, CA). The negative controls were processed with the same procedure except that normal rabbit serum was used in place of the primary antibody. The results of immunohistochemical staining were expressed in two ways: 1) the intensity of staining: +: 10-30% of tumor cells in the section were positive; ++: 30-60% of tumor cells were positive; +++: 60-100% of tumor cells were positive; and 2) the percentage of positive staining = (the numbers of positive samples / the numbers of samples tested) x 100%.

2.4. Double immunohistochemical staining

Twenty-five samples of tumor tissue were processed for double immunohistochemical staining with antibodies to ECM1 followed by mouse monoclonal antibodies to human PCNA and CD34. Frozen sections were used for the CD34 staining because the antibody does not recognize paraffin embedded specimens. For staining, the sections were first incubated with a mixture of rabbit anti-human ECM1 (1:400) and mouse anti-human PCNA (1:500) or mouse anti-human CD34 (1:500) at 4°C overnight. After washing with phosphate buffer saline (PBS), the slides were incubated with peroxidase labeled anti-rabbit IgG and alkaline phosphatase labeled anti-mouse IgG at room temperature for one hour followed

6

by AEC as a peroxidase substrate (red color) and BCIP/NBT as an alkaline phosphatase substrate (blue color). The positive staining for CD34 or PCNA in 10 random fields in either ECM1 positive or negative tumors or regions were highlighted and assessed by a computer image analysis system [6]. To evaluate the extent of vascularization, the outer circumferences of the blood vessels (stained CD34) in a specified region were summed and the results were expressed as the vessel length index as follows: vessel length index = {(total outer vessel length stained with CD34 / measured area) x 100 %}. To evaluate cell proliferation, the index was calculated as follows: PCNA positive frequency = {(number of PCNA positive cells / 400 cells counted) x 100 %}.

2.5. Western Blotting

Frozen samples of human breast tumor tissues (5 invasive duct carcinomas, 1 ductal hyperplasia and 1 normal breast tissue) were analyzed by Western blotting. For this, the samples of tumor tissue were rapidly frozen in liquid nitrogen, ground into a powder and then extracted with 1 ml of lysis buffer (1% Triton X-100, 0.5% Na deoxycholate, 0.5 μg/ml leupetin, 1 mM EDTA, 1 μg/ml pepstatin and 0.5 mM phenylmethylsulfonyl fluoride). The protein concentration of the lysate was determined by the BCA method (Pierce, Rockford IL) and 30 μg of protein was loaded onto 10 % PAGE gel, electrophoresed and transferred to a nitrocellulose membrane. The loading and transferring of equal amounts of protein were confirmed by staining of the membrane with a solution of Ponceau S (Sigma, St. Louis MO). The membranes were blocked with 5% fat-free milk in phosphate buffer saline (PBS, pH 7.4) for 30 min and then incubated with rabbit anti-ECM1-b (1:2,000) overnight at 4°C. After washing, the membrane was incubated with alkaline phosphatase labeled secondary antibody for one hour, followed by a chemo-luminicent substrate and exposed to ECL Hyperfilm MP (Amersham, Piscataway, NJ).

2.6. Statistical Analysis

The data were subjected to statistical analysis using X^2 test or Student's t test. P values <0.05 were considered to be statistically significant.

3. Results

3.1. Expression of ECM1 in various tumors and tissues

We analyzed a panel of human tissues for ECM1 by immunohistochemical staining. These samples represented a spectrum of conditions ranging from normal (regions adjacent to the tumors) to invasive carcinomas. Representative examples of the staining are shown in Fig. 1.

In the case of normal tissue, the vast majority was negative for ECM1 staining (Fig. 1 A, normal colon mucosa, Fig. 1 D, normal gastric mucosa and Fig. 1 G, lobular mild hyperplasia of the breast). Of the 14 normal tissues examined, 13 demonstrated little or no staining for ECM1. The only positive case was that of normal brain tissue adjacent to a tumor. Thus, it appears that the positive frequency for ECM1 expression in normal tissue is relatively low (7.1%, Table 1).

In case of benign lesions, the frequency of positive staining was also low, but greater than that of normal tissue. As illustrated in Tables 1 and 2, 11.7 % (6/51) of the benign tissues were considered to be ECM1 positive. This includes 1 out of 11 cases of breast ductal and lobular hyperplasia; 1 out of 11 cases of breast fibroadenomas; 1 out of 1 case of esophagus squamous proliferation; 1 out of 2 cases of colon adenoma; 1 out of 3 cases of prostate hyperplasia; and 1 out of 10 cases of astrocytoma (Table 2). No ECM1 staining was observed in benign lesions of other tissues, such as meningioma, hemangioblastoma, uterus leiomyoma and mediastinum neurofibroma (Table 2). Statistically, there was no difference between normal tissues and benign lesions with regard to the frequency of ECM1 staining (P>0.05).

In the case of malignant lesions, 72.6% (106/146 cases) were ECM1 positive, including 105 out of 140 cases of carcinoma (75.0%) and 1 out of 6 cases of sarcoma (16.6%, Table 1). There was a significant difference in the ECM1 positive staining frequency between the benign lesions and malignant

8

lesions (P<0.001), as well as between carcinomas and sarcomas (P<0.001). However, there was no correlation between the ECM1 positive frequency and the histological type or degree of differentiation of the cancer tissues studied.

As shown in Table 2, within individual tumors, ECM1 positive staining was heterogeneous. We found that a large proportion of positive slides were evaluated as + in which 10-30% of the cells stained, followed by ++ (30-60%) and finally +++ (60-100%), indicating that even within the same section, the expression level of ECM1 differs considerably, with some cells expressing a significant level of ECM1 while others expressing none. The clinical significance of this heterogeneity with regard to ECM1 expression remains to be evaluated.

3.2. Differences in ECM1 expression between metastatic and non-metastatic tumors

To determine if tumor cells that express ECM1 were preferentially able to give rise to metastases, we stained a panel of paired cancer sections, consisting of the primary tumors from individuals with or without lymph node metastases, collected from patients with breast cancer (13 cases) or lung cancer (20 cases). As shown in Table 3, 33.3% (3/9) of breast cancers without lymph node metastases were positive for ECM1, while 76.9% of those with lymph nodes metastasis were positive (10/13). In addition, 84.6% of the lymph node metastatic breast cancers were ECM1 positive (11/13). In one case, we found that while ECM1 was not expressed in the primary tumor, it was strongly expressed in its lymph node metastases (Fig. 2 A and B). A similar tendency was observed in lung cancer. Lung tumors without metastasis had a low frequency (20.0%) of ECM1 staining, while primary lung tumors with lymph node metastasis had a relatively high frequency (55.0%) (11/20). Statistical analysis showed there were significant differences between the two groups of cancer with and without lymph node metastasis (P<0.05), suggesting that the tumor cells that express ECM1 may have a greater potential to metastasize than those that do not express this protein.

3.3. Correlation of ECM1 expression with CD34 and PCNA

In previous studies, we had found that ECM1 could stimulate the proliferation of some cultured cells and could promote angiogenesis on the CAM of chicken embryos [6]. To determine if similar effects could be observed with tissue specimens, we examined the correlation between these factors in 25 tumor samples (10 breast invasive ductal carcinomas, 8 gastric adenocarcinomas, 6 colon carcinomas and 1 case of esophageal carcinoma). For this study, the sections were stained for both ECM1 and CD34 (a marker for endothelial cells) or PCNA (a marker for cell proliferation). As shown in Figure 3, there was no difference in the vascularization (as measured by blood vessel length index) between regions of the tumors that were ECM1 positive versus those that were negative in the same sections. Similarly, there was no obvious difference between ECM1 positive and negative tumors from different patients with regard to vascularization.

However, there did appear to be a positive correlation between ECM1 expression and cell proliferation. As shown in Fig. 3 G, the double staining revealed that PCNA positive frequency was 72% in ECM1 positive cases, while only 47% in ECM1 negative cases. The differences between these two groups were significant (P<0.05), indicating that ECM1 was indeed correlated with cell proliferation *in vivo*.

3.4. Western blotting for ECM1 in human breast cancer tissues

As described in the introduction, ECM1 comes in both a full length form (ECM1a, 68 kDa) and a truncated form (ECM1b, 46 kDa) and cannot be distinguished by the polyclonal antibody that we use. To determine which of these forms is present in the tumors, we analyzed both normal and invasive ductal carcinoma by Western blotting. Figure 4 shows that human breast carcinomas expressed the full length form of ECM1a and this was much higher than that in normal breast tissues. These results also suggest that Western blotting is more sensitive than immuno-histochemical staining, with regard to sensitivity for detecting ECM1.

4. Discussion

The major conclusion of this study is that ECM1 is upregulated in a distinct subset of tumors. As shown in Table 2, ECM1 staining was positive in 83% of invasive ductal carcinomas of the breast, 73% of squamous cell carcinomas of the esophagus, 88% of adenocarcinomas of the stomach, 78% of adenocarcinomas of the colon and 75% of lung carcinomas. Overall, the average positive frequency in carcinomas was 75.0%, which was much higher than that of sarcomas (16.6%), epithelial hyperplasia (11.7%) and normal tissues (7.1%). These results suggest that although ECM1 may not be a tumor specific protein, its expression levels are significantly elevated in malignant epithelial tumors. The difference in the expression levels of ECM1 between normal tissues (benign lesions) and carcinomas is readily detected by immunohistochemical staining, which can be used as a marker for cancer tissue. Further studies are required to evaluate the diagnostic value of ECM1 staining in a clinical setting.

The most interesting finding of this study is that ECM1 is preferentially expressed by tumors that give rise to metastases. This was indicated by the fact that the frequency of positive staining was higher in tumors with such metastases as compared to tumors that had not spread from the primary site (Table 3). Furthermore, analysis of the metastases themselves revealed a high frequency of ECM1 staining. It should be noted that in the primary tumors tested, the expression of ECM1 was very heterogeneous. Even within the same section, some areas stained strongly for ECM1, while other areas showed weak or no staining. A large portion of tumors were classified as "+" in which 10-30% of the tumor cells demonstrating positive staining. The cells that express ECM1 may represent a more aggressive and malignant phenotype in comparison to those that do not express this molecule.

At this point, we do not know the exact role of ECM1 in tumor development and progression. In a previous study [6], we found that the addition of purified, recombinant ECM1 could stimulate the proliferation of endothelial cells *in vitro* and promoted the formation of new blood vessels in the chorioallantoic membrane of chicken embryos. However, in this study, the results of double-staining for

11

ECM1 and CD34 did not indicate that there was a correlation between the levels of ECM1 and the degree of angiogenesis. In many of the sections, we noted that although tumor cells expressed high levels of ECM1, it tended to be restricted to the cytoplasm of tumor cells or to peri-cellular regions. It is uncertain whether the ECM1 produced by tumor cells is able to diffuse to areas of pre-existing blood vessels in sufficient concentrations to stimulate angiogenesis. It is also possible that ECM1 alone is not sufficient to alter angiogenesis, which may require multiple angiogenic factors.

The expression of ECM1 was correlated with rapid cell division, as suggested by the double staining of ECM1 and PCNA, an index for cell proliferation. There was a higher frequency of PCNA staining in regions of the tumor that were positive for ECM1 staining than in areas than were negative. Thus, rapidly proliferating cells express greater amounts of the ECM1. While we only demonstrated that a correlation exists, it is possible that ECM1 may contribute to this increased proliferation through an autocrine mechanism.

Another finding of this study was that there was a high frequency of ECM1 staining in squamous cell cancers (73%) as well as in normal proliferating squamous epithelium. Indeed, the normal squamous esophageal epithelium adjacent to tumors stained strongly for ECM1. This may be related to the fact that ECM1 is involved in the differentiation of epithelial cells, as suggested by the fact that ECM1 is expressed in adult human skin and the gene for ECM1 is located close to the epidermal differentiation complex [4]. Furthermore, loss-of-function mutations of ECM1 leads to lipoid proteinosis (Urbach-Wiethe disease) typified by generalized thickening of skin, mucosae and certain viscera [8-14], suggesting that ECM1 plays a role in maintaining the normal structure of extracellular matrix in the skin [4]. However, we found that ECM1 was not detected in most normal non-squamous epithelium, such as ductal or lobular epithelium of the breast and adenoepithelium of the stomach, colon and lung. It appears that when these cells transform into malignant tumor cells, the expression of ECM1 is up-regulated. Thus, ECM1 may be of diagnostic or prognostic value in adenocarcinomas, but not in squamous cell carcinomas.

In conclusion, the results of this study indicate that ECM1 is over-expressed in some carcinomas, particularly those that were metastatic. If ECM1 expressing cells in primary tumors preferentially undergo metastasis, then this may be a useful index to evaluate clinical prognosis.

REFERENCES

[1] E. Mathieu, L. Meheus, J. Raymackers, J. Merregaert, Characterization of the stromal osteogenic cell line MN7: Identification of secreted MN7 proteins using two-dimensional polyacrylamide geleclectrophoresis, Western blotting and micro-sequencing. J. Bone Min. Research, 9 (1994) 903-913.

[2] J. Bhalerao, P. Tylzanowski, J.D. Filie, C.A. Kozak, J. Merregaert, Molecular cloning, characterization, and genetic mapping of the cDNA coding for a novel secretory protein of mouse. Demonstration of alternative splicing in skin and cartilage. J Biol Chem. 270 (1995) 16385-16394.

[3] P. Smits, J. Ni, P. Feng, J. Wauters, W. Van Hul, M.E. Boutaibi, P.J. Dillon, J. Merregaert, The human extracellular matrix gene 1 (ECM1): genomic structure, cDNA cloning, expression pattern, and chromosomal localization. Genomics 45 (1997) 487-95.

[4] M.R. Johnson, D.J. Wilkin, H.L. Vos, R.I. Ortiz de Luna, A.M. Dehejia, M.H. Polymeropoulos, C.A. Francomano, Characterization of the human extracellular matrix protein 1 gene on chromosome 1q21. Matrix Biol., 16 (1997) 289-292.

[5] P. Smits, Y. Poumay, M. Karperien, P. Tylzanowski, J. Wauters, D. Huylebroeck, M. Ponec, J. Merregaert, Differentiation-dependent alternative splicing and expression of the extracellular matrix protein 1 gene in human keratinocytes. J. Invest. Dermatol., 114 (2000) 718-724.

[6] Z. Han, J. Ni, P, Smits, C.B. Underhill, B. Xie, Y. Chen, N. Liu, P. Tylzanowski, D. Parmelee, P. Feng, I. Ding, F. Gao, R. Gentz, D. Huylebroeck, J. Merregaert, L. Zhang, Extracellular matrix protein 1 (ECM1) has angiogenic properties and is expressed by breast tumor cells. FASEB 15 (2001) 988-994.

[7] M.M. Deckers, P. Smits, M. Karperien, J. Ni, P. Tylzanowski, P. Feng, D. Parmelee, J. Zhang, E. Bouffard, R. Gentz, C.W. Lowik, J. Merregaert, Recombinant human extracellular matrix protein 1

inhibits alkaline phosphatase activity and mineralization of mouse embryonic metatarsals in vitro. Bone, 28 (2001) 14-20.

[8] T. Hamada, W.H. McLean, M. Ramsay, G.H. Ashton, A. Nanda, T. Jenkins, I. Edelstein, A.P. South, O. Bleck, V. Wessagowit, R. Mallipeddi, G.E. Orchard, P.J. Wan H, Dopping-Hepenstal, J.E. Mellerio, N.V. Whittock, C.S. Munro, M.A. van Steensel, P.M. Steijlen, J. Ni, L. Zhang, T. Hashimoto, R.A. Eady, J.A. McGrath, Lipoid proteinosis maps to 1q21 and is caused by mutations in the extracellular matrix protein 1 gene (ECM1). Hum Mol Genet., 11 (2002) 833-840.

[9] E. Urbach and C. Wiethe, Lipoidosis cutis et mucosae. Virchows Arch. Path. Anat. 273 (1929) 285-319.

[10] P. Hofer, Urbach-Wiethe disease (lipoglycoproteinosis; lipoid proteinosis; hyalinosis cutis et mucosae). A review. *Acta. Dermatovenereol.* 53 (suppl.) 71 (1973) 1-52.

[11] G. Findlay, F.P. Scott, D.J. Cripps, Porphyria and lipid proteinosis. Br. J. Dermatol. 78 (1966) 69-80.

[12] S. Dinakaran, S.P. Desai, I.R. Palmer, M.A. Parsons, Lipoid proteinosis: clinical features and electron microscopic study. Eye 15 (2001) 666-668.

[13] D.R. Olsen, M.L. Chu, J. Uitto, Expression of basement membrane zone genes coding for type IV procollagen and laminin by human skin fibroblasts in vitro: elevated alpha 1 (IV) collagen mRNA levels in lipoid proteinosis. J. Invest. Dermatol. 90 (1988) 734-738.

[14] R. Fleischmajer, T. Krieg, M. Dziadek, D. Altchek, R. Timpl, Ultrastructure and composition of connective tissue in hyalinosis cutis et mucosae skin. J. Invest. Dermatol. 82 (1984) 252-258.

FIGURE LEGENDS

Fig. 1. Immunohistochemical staining of ECM1 in various normal and tumor tissues. Paraffin sections were stained for ECM1 with affinity purified rabbit antibodies (1:400) followed by peroxidase labeled secondary antibodies and finally a peroxidase substrate (AEC) that gives a red precipitate and counter-stained with hematoxylin. The representative pictures were taken (A, B, C, D, E, G, H, K L, M) at 75 x or (F, I, J) at 150 x magnification. **A)** Normal colon mucosa with little or no staining of ECM1; **B)** Colon tubular adenocarcinoma showing ++ ECM1 staining; **C)** Large bowel adenoma, + ECM1 staining; **D)** Gastric mucosa, negative for ECM1; **E)** Gastric tubular cancer, ++ ECM1 staining; **F)** Poorly differentiated adenocarcinoma, +++ ECM1 staining; **G)** Mild lobular hyperplasia of the breast showing little or no expression of ECM1; **H and I)** Invasive ductal carcinomas of the breast with ++ to +++ ECM1 staining; **J)** Prostate adenocarcinoma with + ECM1 staining; **K)** Lung squamous cell carcinoma with + ECM1 staining; **L)** Lung adenocarcinoma with + ECM1 staining; and **M)** Squamous cell cancer of the esophagus with ++ ECM1 staining.

Fig. 2. ECM1 in paired samples of primary and metastatic tumors. Paired sections of primary and secondary tumors collected from same patient with either breast or lung cancer and stained for ECM1. The representative pictures were taken at 75 x magnification. **A and B)** A primary breast cancer shows little or no ECM1 staining while a metastasis in the lymph node from same patient demonstrates ECM1 ++ staining. **C and D)** A primary lung cancer shows ECM1 ++ staining while it metastasis to a lymph node shows ECM1 ++ staining.

Fig. 3. Double staining of ECM1 and CD34 or PCNA. The sections were incubated at 4°C overnight with a mixture of rabbit antibodies to ECM1 and mouse monoclonal antibody to PCNA or CD34. After washing, the sections were incubated with peroxidase-labeled anti-rabbit IgG and alkaline phosphatase-

labeled anti-mouse IgG followed by AEC as a peroxidase substrate (red color for ECM1) and NBT/BCIP as peroxidase substrate (blue color for CD31 or PCNA). The positive staining were analyzed using an image analysis system. The results were expressed as vessel length index or PCNA positive frequency (see material and method). The representative pictures were taken at 75 x magnification. **A)** The vessels (in blue) in an ECM1 positive (in red) breast cancer. **B)** The vessels (in blue) in an ECM1 negative breast cancer are shown. **C)** The vessels (in blue) in an ECM1 positive (in red) colon adenocarcinoma are shown. **D)** The vessels (in blue) in an ECM1 negative colon adenocarcinoma are demonstrated. **E)** Comparison of the vessel length index (a measure of vasularization see Materials and Methods) in sections with ECM1 positive and negative areas (heterogeneous staining) and sections that were completely negative ECM1 indicates that there were no differences between the three groups (P>0.05). **F)** Double-staining of a breast cancer for ECM1 (in red) and PCNA (in blue) is shown. **G)** Comparison of PCNA positive frequency between ECM1-positive and ECM1-negative tumors indicates that proliferation was higher in ECM1 positive cells than in ECM1 negative cells (P<0.05).

Fig. 4. Western Blotting for ECM1. Samples of breast cancer tissue lysate containing 30 μg of protein were loaded onto 10% PAGE gels, electrophoresed and transferred to nitrocellulose membranes. The membranes were blocked with 5% fat free milk and then incubated with rabbit anti-ECM1 (1:2,000) at 4°C overnight. After washing, the membrane was incubated with an alkaline phosphatase labeled secondary antibody for one hour, followed by a chemo-luminicent substrate and exposure to ECL Hyperfilm MP. **A)** The Western blot shows that a band at 68 kDa corresponding to ECM1a is present in all of the tissue extracts, but is expressed to a greater extent in the breast cancer tissues as compared to normal tissue. **B)** Comparison of density of 68 kDa band shows a significant higher level of ECM1 in breast cancer tissues than that in the normal breast tissue (P<0.05).

Table 1. Expression of ECM1 in Different Histological Lesions

Histological type	Number of Cases	Positive Cases	Negative Cases	Positive Rate (%)
Malignant tumor	146	106	40	72.6
Carcinoma	140	105	35	75.0
Sarcoma	6	1	5	16.6
Benign lesions	51	6	45	11.7
Epithelium	31	5	26	16.1
Non-epithelium	20	1	19	5
Normal tissues	14	1	13	7
Total	211	113	98	53.6

Table 2. Immunohistochemic Staining of ECM1 in Various Tumors and Tissues

Histological type	Number of cases	Positive staining +++	++	+	Negative Cases	Positive Cases	Positive Rate (%)
Breast							
Normal breast lobular	4				4	0/4	0
Fibroadenoma	11			1	10	1/11	9
Ductal and lobular hyperplasia	11			1	10	1/11	9
Invasive ductal carcinoma	37	3	4	24	6	31/37	83
Esophagus							
Squamous cell cancer	26		3	16	7	19/26	73
squamous hyperplasia	4			1	3	1/4	25
Gastric cancer (total)	26		3	16	3	23/26	88
Papillary	1				1	0/1	
Tubular	11		4	7		11/11	
Poorly	12		3	8	1	11/12	
Mucinous	2			1	1	1/2	
Non-cancerous gastric mucosa	4				4	0/4	
Large bowel cancer (total)	32	1	7	17	7	25/32	78
Well differentiation	15		4	9	2	13/15	
Moderately differentiation	8	1	1	5	1	7/8	
Poorly differentiation	5		2	2	1	4/5	
Mucinous	4		1		3	1/4	
Large bowel adenoma	2			1	1	1/2	50
Non-cancerous intestinal mucosa	5				5	0/5	0
Gastrointestinal leiomyosarcoma		2			2	0/2	0
Retroperitoneum liposarcoma	1				1	0/1	0
Pancreas ductal carcinoma	2		1	1		2/2	100

Liver cell carcinoma	6			1	5	1/6	16.7
Liver bile duct carcinoma	1			1		1/1	100
Lung cancer (total)	4			3	1	3/4	75
Adenocarcinoma	3			2	1	2/3	
Squamous cell cancer	1			1		1/1	
Renal clear cell carcinoma	3				3	0/3	0
Prostate hyperplasia	3			1	2	1/3	33
Prostate adenocarcinoma	3			3		3/3	100
Brain tumor (total)	18			2	16	2/18	11
Astrocytoma	10			1	9	1/10	
Glioblastom	2			1		1/2	
Meningioma	3				3	0/3	
Hemangioblastoma	1				1	0/1	
Non-tumorous brain tissue	1			1		1/1	
Mediastinum neurofibroma	3				3	0/3	0
Uterus leiomyoma	2				2	0/2	0
Total	211	4	22	90	95		

Table 3. Differences between cancers with and without lymph node metastasis with regard to

ECM1 expression

Histopathology Type	Total Case	Positive Cases	Positive Staining +	Positive Staining ++	Negative Cases	Positive (%)	P Value*
Breast cancer							
+ Lymph node metastasis	13	10	2	8	3	76.9	<0.01
- Lymph node metastasis	9	3	1	2	6	33.3	-
Lymph node metastasis	13	11	7	4	2	84.6	<0.01
Lung cancer							
+ Lymph node metastasis	20	11	7	4	9	55.0	<0.01
- Lymph node metastasis	10	2	1	1	8	20.0	-
Lymph node metastasis	20	7	3	4	13	35.0	<0.05
Total Cases	85	44	31	13	41	51.8	

*: X^2 test was conducted to compare the expression rate of ECM1 between cancers with and without

lymph node metastasis.
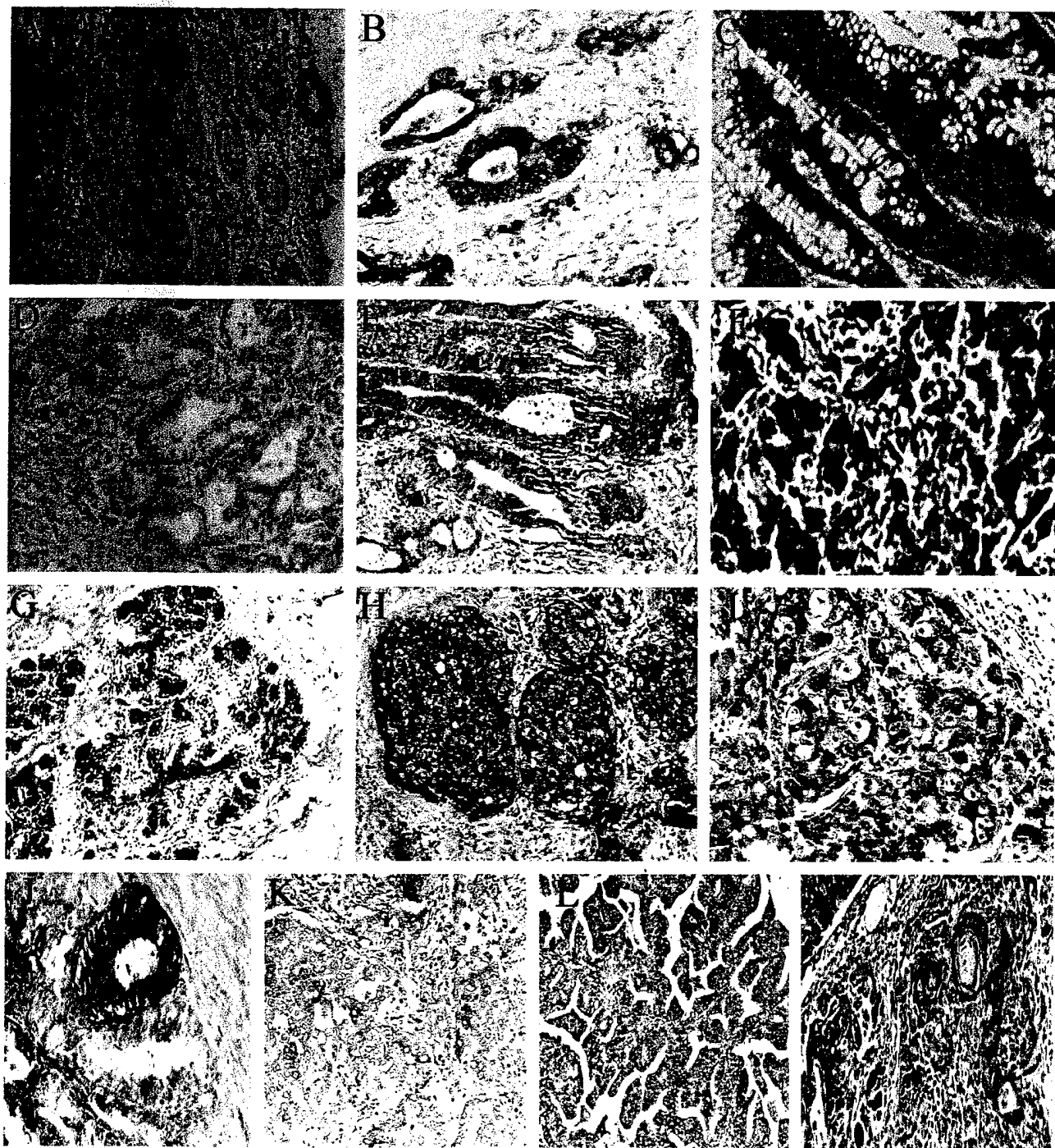
Figure 1, Wang, et al
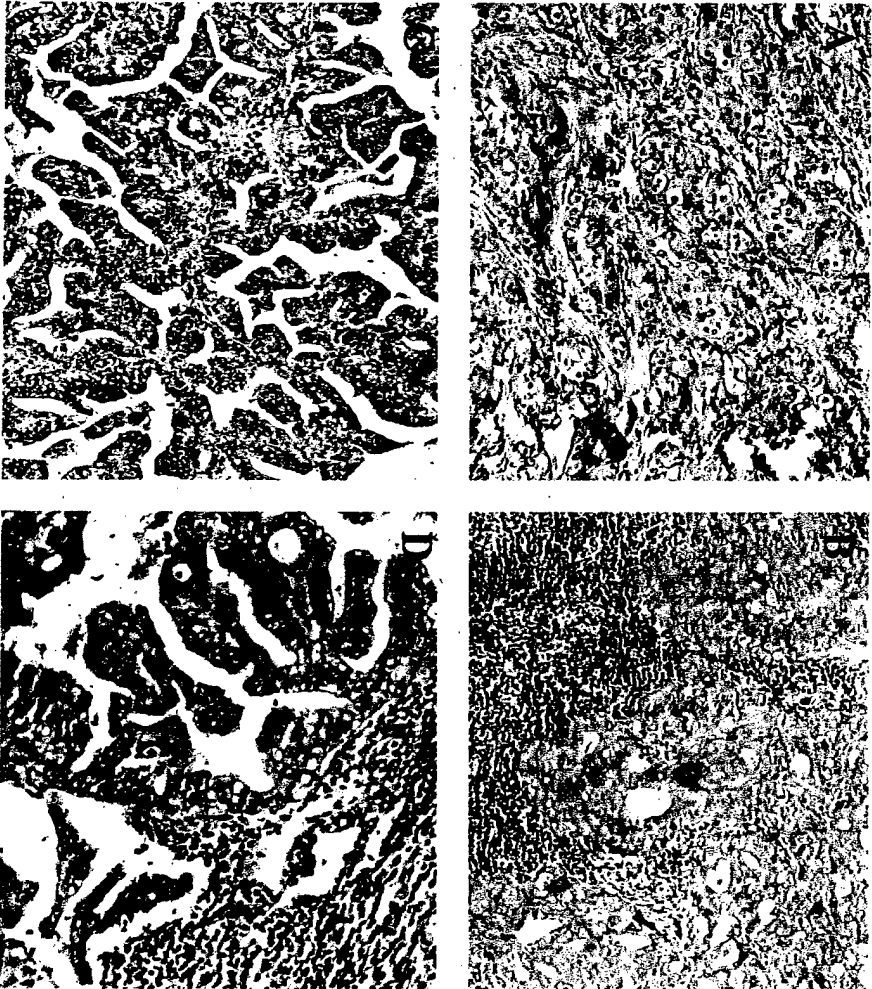
Figure 2, Wang, et al

Figure 3, Wang, et al

A

MW (kDa)

Normal breast tissue

breast cancer_tissues

1   2   3   4   5

68 —

46 —

Protein loading control
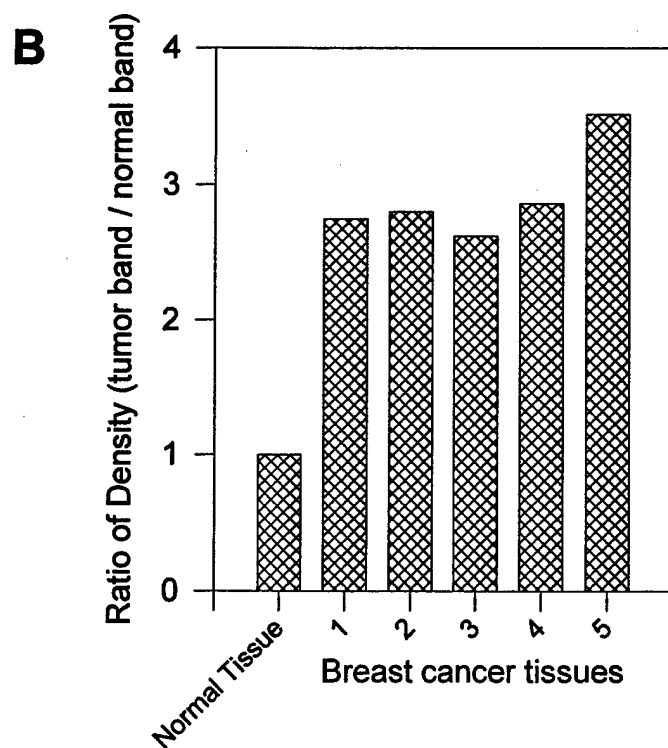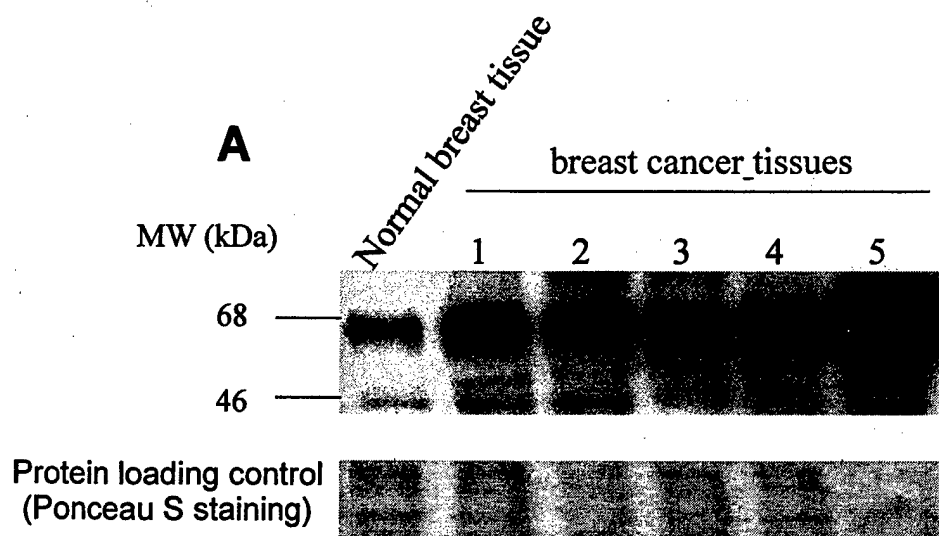(Ponceau S staining)

B
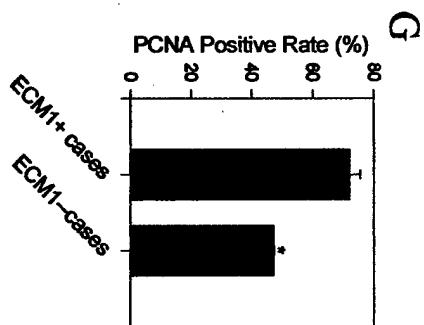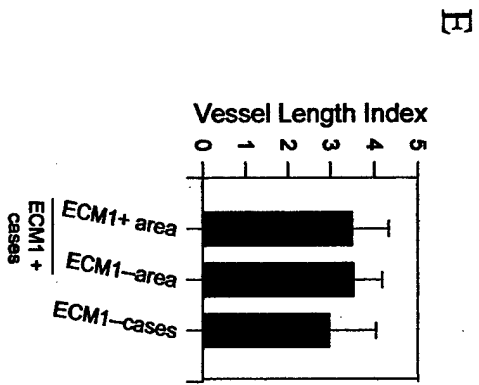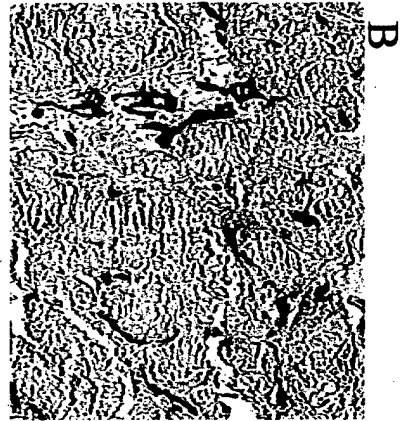
Figure 4, Wang, et al

Triptolide Inhibits the Growth and Metastasis of Solid Tumors[1]

Shanmin Yang, Jinguo Chen, Zhen Guo,
Xue-Ming Xu, Luping Wang, Xu-Fang Pei, Jing Yang,
Charles B. Underhill, and Lurong Zhang[2]

Department of Oncology, Georgetown University Medical Center,
Washington, DC 20007 [S. Y., J. C., X-M. X., L. W., X-F. P., J. Y.,
C. B. U., L. Z.], and Key Laboratory of China Education Ministry on Cell
Biology and Tumor Cell Engineering, Xiamen University, Fujian,
People's Republic of China 361003 [S. Y., Z. G., L. Z.]

Abstract

Triptolide (TPL), a diterpenoid triepoxide purified from
the Chinese herb *Tripterygium wilfordii Hook F,* was
tested for its antitumor properties in several model
systems. *In vitro,* TPL inhibited the proliferation and
colony formation of tumor cells at extremely low
concentrations (2–10 ng/ml) and was more potent than
Taxol. Likewise, *in vivo,* treatment of mice with TPL for
2–3 weeks inhibited the growth of xenografts formed
by four different tumor cell lines (B16 melanoma, MDA-
435 breast cancer, TSU bladder cancer, and MGC80-3
gastric carcinoma), indicating that TPL has a broad
spectrum of activity against tumors that contain both
wild-type and mutant forms of p53. In addition, TPL
inhibited experimental metastasis of B16F10 cells to
the lungs and spleens of mice. The antitumor effect
of TPL was comparable or superior with that of
conventional antitumor drugs, such as Adriamycin,
mitomycin, and cisplatin. Importantly, tumor cells
that were resistant to Taxol attributable to the
overexpression of the multidrug resistant gene 1 were
still sensitive to the effects of TPL. Studies on cultured
tumor cells revealed that TPL induced apoptosis and
reduced the expression of several molecules that
regulate the cell cycle. Taken together, these results
suggest that TPL has several attractive features as a
new antitumor agent.

Introduction

TPL[3] is a diterpenoid triepoxide (M_r 360) derived from the
herb *Tripterygium wilfordii* that has been used as a natural
medicine in China for hundreds of years (1). TPL exerts both
anti-inflammatory and antifertility activities through its ability
to inhibit the proliferation of both activated monocytes and
spermatocytes (2–8).

Several reports have indicated that TPL also inhibits the
proliferation of cancer cells *in vitro* and reduces the growth of
some tumors *in vivo* (9–12), *e.g.,* Shamon *et al.* (10) have
found that TPL can block the growth of human mammary
tumor cells in nude mice, and similarly, Tengchaisri *et al.* (11)
have reported that it will inhibit the growth of cholangiocar-
cinoma cells in hamsters. In addition, clinical trials in China
have demonstrated that TPL could achieve a total remission
rate of 71% in mononuclocytic leukemia and 87% in gran-
ulocytic leukemia, which was more effective than any other
chemotherapeutic agent currently available (13). Studies on
cells grown in tissue culture suggest that TPL may be induc-
ing apoptosis by altering pathways involving the proteins p21
and p53 (9, 12). However, at this point, the exact mechanism
by which TPL is able to inhibit tumor cell growth remains
unknown. In addition, TPL has not been characterized with
regard to its effects on different types of solid tumors.

In this study, we have examined a highly purified prepa-
ration of TPL with regard to its activity against a variety of
solid tumors and made the following observations: (*a*) we
found that the antitumor effects of TPL were very broad,
because it was able to block the growth of four tumor cells
with distinct origins and of different p53 status (B16 mouse
melanoma, MDA-435 human breast cancer, TSU bladder
cancers, and MGC80-3 gastric cancer); (*b*) we found that the
antitumor effects of TPL were comparable with other con-
ventional chemotherapeutic drugs, such as Adriamycin, mi-
tomycin, and cisplatin; (*c*) we found that TPL was effective
against tumor cells that overexpress the MDR1 and are re-
sistant to the effects of other chemotherapeutic compounds,
such as Taxol; and (*d*) we have found that TPL influences the
expression of key molecules that regulate apoptosis and cell
cycle progression.

Materials and Methods

Cell Lines. B16F10 mouse melanoma cells, MDA-435 hu-
man breast carcinoma, and TSU human bladder cancer cells
were obtained from the Tumor Bank of the Lombardi Cancer
Center at Georgetown University (Washington, DC).
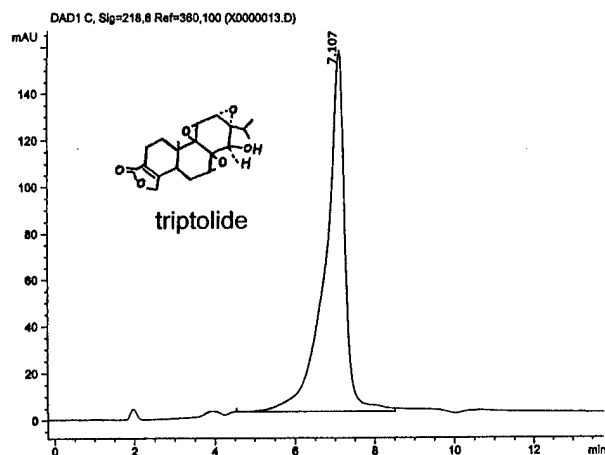MGC80-3 human gastric carcinoma cells were obtained from

Fig. 1. The purity of TPL as assessed by HPLC. The preparation of TPL was applied to a Hypersil C18 column (reverse phase) and eluted with solution of acetonitrile and water. The single peak indicated that the preparation was >99% pure. The structure of TPL is also shown.

the Cancer Research Center of the Life Science School at Xiamen University (People's Republic of China). The tumor cells were cultured in 10% calf serum and 90% DMEM.

Source of TPL. The TPL used in these experiments was obtained from Fujian Institute of Medical Science. The purification was carried out using a modification of the procedure described by Kupchan *et al.* (1). Briefly, the ground roots of *Tripterygium wilfordii Hook F* were extracted with ethanol, evaporated, and partitioned with diethyl ether/ethyl acetate/ water. The ester layer was subjected to column chromatography on silica gel and eluted with methanol-chloroform. The eluted fractions were evaporated, and the residue was re-chromatographed on silica gel and eluted with diethyl ether. TPL was obtained from the later-eluting fractions. The purity of the TPL was assessed by HPLC on a Hypersil C18 column using acetonitrile-water (40:60, volume for volume) as the mobile phase (14). As shown in Fig. 1, the TPL eluted as a single peak and on this basis was determined to be >99% pure. The purified TPL was dissolved at a concentration of 1 mg/ml in a mixture of 60% ethanol, 30% DMSO, and 10% phosphate buffer (pH 6.0) as recommended by Mao *et al.* (15).

Cell Proliferation Assay. Aliquots of complete medium containing 1.5×10^4 cells (MDA-435, B16F10, or TSU cells) were distributed into 96-well tissue culture plates. On the following day, the media were replaced with 190 μl of fresh media and 10 μl of a solution containing different concentrations of the TPL or Taxol at 100 ng/ml. Three days later, 30 μl of 0.3 μCi [^{3}H]thymidine in serum-free media were added to each well. After 12 h, the cells were harvested on a glass filter with a 96-well auto-harvester, and the amount of incorporated [^{3}H]thymidine was determined with a β-counter.

Colony Formation Assay. The viability of the tumor cells was determined by staining with trypan blue followed by visual examination on a hemocytometer. B16F10 cells were suspended at a concentration of 2×10^4 cells/ml in 0.36% agarose in 10% calf serum and DMEM containing TPL (0, 2,

or 10 ng/ml) and then immediately placed on top of a layer of 0.6% solid agarose in 10% calf serum and DMEM medium in six-well plates. Two weeks later, the number of colonies >60 μm in diameter was determined using an Omnicon Image Analysis System (Imaging Products, Chantilly, VA).

Effect of TPL on the Growth of Primary Tumors in Mice. Four tumor cell lines were used to establish primary tumor xenografts. The B16F10 cells (5×10^5 cells/site, 10 mice/ group) were injected s.c. into 6-week-old C57BL/6 mice and allowed to grow for 3 days. For studies involving human tumor cells, such as TSU, MDA-435, or MGC80-3, the cells were injected s.c. into the flanks of 5–6-week-old BABL/c nude/nude mice (5×10^6 cells/site, 8 mice/group). After growing for 3 days, the tumor xenografts reached a size of ~100 mm^3. Thereafter, TPL (0.15 mg/kg/day) was injected i.p. into the mice on a daily basis. At the end of 2 or 3 weeks, the mice were sacrificed, and the tumor xenografts were removed, photographed, and weighed.

Effect of TPL on Experimental Metastases in Mice. To examine the effects of TPL on experimental metastasis, B16F10 cells (5×10^4 cells in serum-free DMEM) were injected into the tail veins of mice (5-week-old C57BL/6, 10 mice/group). After 3 days, TPL (0.15 mg/kg/day) was administered daily to the mice by i.p. injections. Two weeks later, the mice were sacrificed, and the lung and spleen metastases were photographed and counted under a dissecting microscope in a double blind setting.

Comparison of TPL with Conventional Chemotherapeutic Drugs. For the *in vitro* comparison of drug potency, MGC80-3 cells were cultured in a 96-well plate and then treated with the following agents: (*a*) vehicle alone (control); (*b*) TPL at a concentration of 10 ng/ml (28 nM); (*c*) Adriamycin at 360 ng/ml (663 nM); (*d*) mitomycin at 2700 ng/ml (8.1 μM); and (*e*) cisplatin at 2490 ng/ml (8.3 μM). Two days later, the viability of the cells was determined by the MTT method according to the manufacturer's instructions (Sigma Chemical Co., St. Louis, MO). For the *in vivo* comparison of drugs, mice with tumor xenografts (100 mm^3 in size) were divided into five groups (5 mice/group) and treated as follows: (*a*) vehicle alone (PBS); (*b*) TPL at 0.25 mg/kg daily; (*c*) Adriamycin at 1.2 mg/kg weekly; (*d*) mitomycin at 1.7 mg/kg weekly; and (*e*) cisplatin at 7 mg/kg weekly. The doses and injection regimens for these chemotherapeutic reagents were based on reports published previously (16). Three weeks later, the mice were sacrificed, and the tumors were dissected and weighed. The data were expressed as:

Inhibition % = [1 − (mean weight of tumor tests/mean weights of tumor controls)] × 100%.

Effect of TPL on Tumor Cells Overexpressing MDR1. A pair of MDA-435 cell lines that had been transduced with either a control retrovirus vector or one containing the *MDR1* was kindly provided by Dr. Clarke of the Lombardi Cancer Center (17). These cells were tested for their sensitivities to TPL in both *in vitro* proliferation assays and colony formation assays and *in vivo* tumor growth using the procedures described above.

Detection of DNA Fragmentation. The induction of apoptosis in the cultured cells was determined by analysis of DNA fragmentation. For this, 2×10^5 TSU cells were grown

to 80% confluence on tissue culture plates and then incubated in the presence and absence of 10 ng/ml TPL for 3 days. The DNA was extracted and subjected to gel electrophoresis according to the methods of Sellins and Cohen (18). The resulting gel was stained with ethidium bromide and photographed under a UV lamp.

Western Blotting. Cultures of MDA-435 cells at 80% confluence in 100-mm dishes were treated with TPL (2 or 10 ng/ml) for different lengths of times and then harvested with 1 ml of lysis buffer (1% Triton X-100, 0.5% Na deoxycholate, 0.5 μg/ml leupetin, 1 mM EDTA, 1 μg/ml pepstatin, and 0.5 mM phenylmethylsulfonyl fluoride). The protein concentration of the lysate was determined by the bicinchoninic acid method (Pierce, Rockford, IL), and 30 μg of protein were loaded onto a 10% SDS-PAGE, electrophoresed, and transferred to a nitrocellulose membrane. The loading and transferring of equal amounts of protein were confirmed by staining the membrane with a solution of Ponceau S (Sigma). The membranes were blocked with 5% fat-free milk in PBS (pH 7.4) for 30 min and then incubated overnight with 0.2 μg/ml of the different antibodies (Oncogene, Boston, MA). After washing, the membranes were incubated with alkaline phosphatase-labeled secondary antibodies for 1 h, followed by a chemo-luminicent substrate, and exposed to enhanced chemiluminescence Hyperfilm MP (Amersham, Piscataway, NJ).

Statistical Analysis. The mean and SE were calculated from the raw data and then subjected to Student's t test. A $P < 0.05$ was regarded as statistically significant.

Results

Effect of TPL on the Proliferation of Tumor Cells *in Vitro*.

The TPL was extracted from the roots of *Tipterygium wilfordii* and purified by chromatography on silica gel. Analysis of the preparation by reverse-phase HPLC revealed a single peak (Fig. 1), indicating that it was ≥99% pure. In initial experiments, we examined the effects of different doses of TPL on the proliferation of tumor cells (MDA-435, TSU, or B16) in tissue culture. As shown in Fig. 2A, after 2 days of treatment, the proliferation of the tumor cells was significantly inhibited by TPL in a dose-dependent manner as indicated by [^{3}H]thymidine incorporation. This was also reflected in the fact that the treated tumor cells had an unhealthy appearance in that they were round, condensed, and detached as compared with the controls (data not shown). Significantly, the inhibitory effect of TPL at 25 ng/ml (70 nM) was stronger than that of Taxol at 100 ng/ml (117 nM), suggesting that TPL is very potent. The inhibition rate increased in a time-dependent manner, and the maximum effect was observed at days 3–4 after treatment with 2 ng/ml TPL (data not shown).

TPL also influenced colony formation of several types of tumor cells in soft agar, which is one of the best *in vitro* indicators of malignant behavior. As shown in Fig. 2B, treatment of B16F10 tumor cells with TPL (2 or 10 ng/ml) resulted in fewer and smaller colonies than those treated with vehicle control. In addition, Taxol at a concentration of 100 ng/ml resulted in a 60% inhibition rate, whereas TPL at 2 ng/ml had an 80% inhibition rate, again indicating that TPL is very potent.
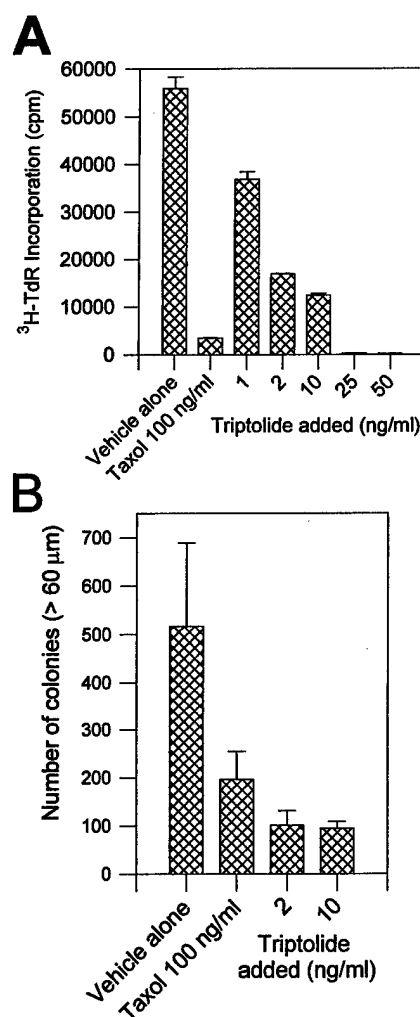
Fig. 2. Effect of TPL on proliferation and colony formation of tumor cells. In *A*, MDA-435 tumor cells were treated with vehicle alone, 100 ng/ml Taxol, or TPL at the indicated concentrations for 2 days, and then [^{3}H]thymidine was added to the cultures for 12 h. The cells were harvested, and the amount of incorporated [^{3}H]thymidine was determined with a β-counter. The proliferation of the tumor cells was inhibited by TPL in a dose-dependent manner ($P < 0.01$). Similar results were obtained with B16F10 and TSU cells. In *B*, B16F10 tumor cells were suspended in 0.36% agarose containing Taxol or TPL at the indicated concentrations. Two weeks later, the colonies >60 μm were counted with Omnicon Image Analysis system. The colony formation was inhibited by TPL and Taxol ($P < 0.01$). All of the experiments were repeated three times. Similar results were obtained in other tumor cell lines, such as 4T1 and TSU cells.

It should be noted that several components with similar structure to TPL can also be purified from *Tripterygium wilfordii Hook*, such as epitriptolide, triptonide, and triptophenolide (1, 19–21). When we compared the antitumor potency of these compounds, we found that only TPL showed significant activity and that the other three components, even at a 1000-fold higher concentration (10 μg/ml), could not achieve an inhibition as effective as TPL at 10 ng/ml (data not shown).

Effect of TPL on Primary Tumor Xenografts. Next, we examined the effects of TPL on the growth of primary tumor xenografts in mice. In preliminary studies, we found that the
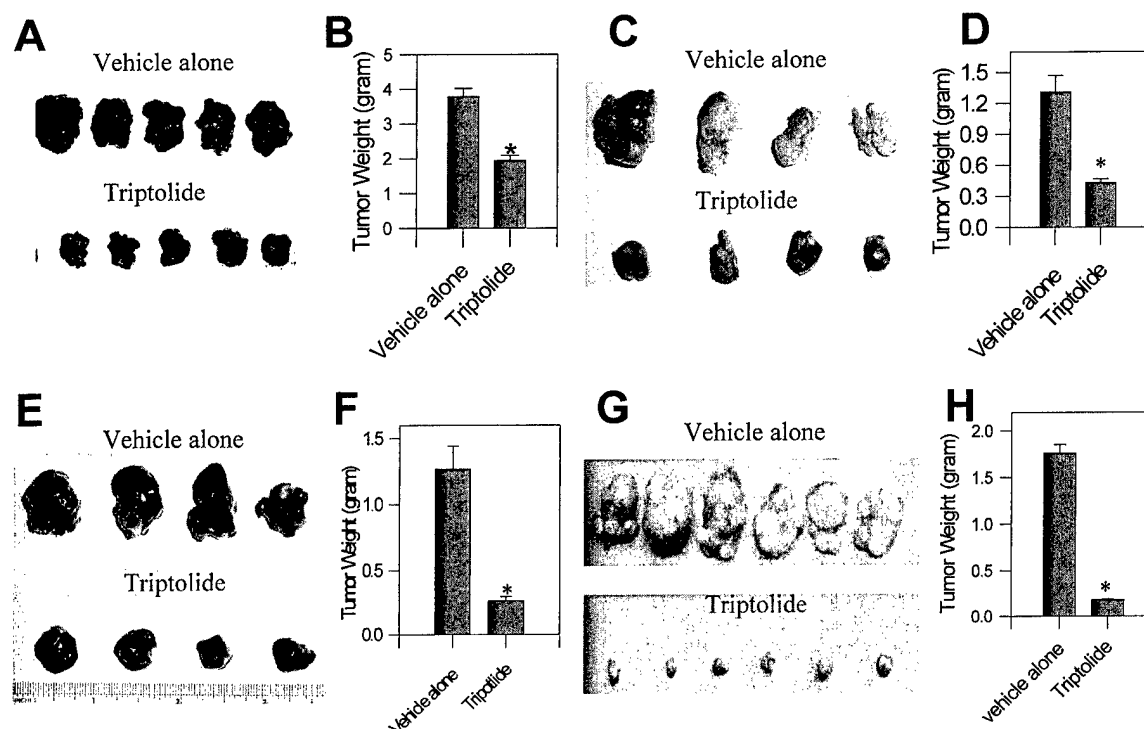
Fig. 3. Effect of TPL on the growth of primary tumors in mice. Mice were injected s.c. with the following tumor cells: (a) B16F10 mouse melanoma (*A* and *B*); (b) TSU human bladder (*C* and *D*); (c) MDA-435 human breast (*E* and *F*); and (d) MGC80-3 human gastric carcinoma (*G* and *H*). Beginning 3 days later, the mice were divided into two groups, one of which was given daily i.p. injections of TPL (0.15 mg/kg/day), whereas the other was given vehicle controls. At the end of 2 or 3 weeks, the mice were sacrificed, and the tumors were removed, photographed, and weighed. The growth of all four types of tumors was inhibited by TPL ($P < 0.01$).

maximum tolerated dose for TPL in mice was 0.25 mg/kg administered daily. On this basis, we chose a dose that was 60% of this maximum tolerated dose or 0.15 mg/kg/day, i.p. The injections were given daily because TPL has a short half-life. This regimen did not appear to adversely affect the mice, because there were no obvious signs of sickness after 2 weeks, and there was no difference in the body weights between groups treated with and TPL and the controls (data not shown).

When the TPL (0.15 mg/kg/day, i.p.) was administered to mice with established tumor xenografts, the results were dramatic. Fig. 3 shows that TPL had a significant inhibitory effect on the growth of all four tumor cell lines (B16 by 50%, MDA-435 cells by 80%, TSU by 65%, and MGC80-3 by 90%). These results suggest that TPL is active against a spectrum of different tumor types, although the sensitivity varies depending on the particular tumor.

Effect of TPL on Experimental Metastases. In the next series of experiments, we tested the ability of TPL to inhibit experimental lung metastases. For this, B16F10 cells were injected into the tail veins of C57BL/6 mice, which were subsequently treated with TPL (0.15 mg/kg/day for 14 days). The mice were then sacrificed, and the organs were examined to determine the number of tumor nodules. As shown in Fig. 4, the number of lung metastases was dramatically reduced in the group treated with TPL as compared with the vehicle control. The B16 cells also metastasized to the

spleen but at a somewhat lower rate than to the lungs. Here again, the treatment with TPL decreased the level of obvious spleen metastases from 40% in the control group as opposed to 18% in the TPL-treated group (data not shown).
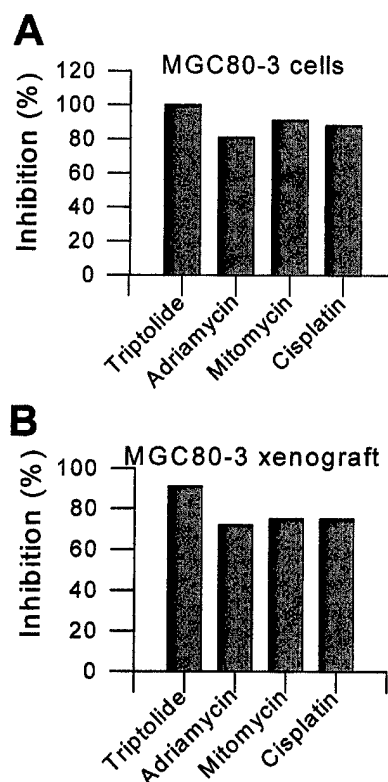
Comparison of TPL with Other Chemotherapeutic Drugs. Next, we compared the efficacy of TPL with that of other chemotherapeutic drugs that are in wide use. Initially, we compared the effects of these drugs on the growth of MGC80-3 tumor cells in tissue culture as determined by the MTT method. After 2 days of treatment, TPL at a concentration of 10 ng/ml (28 nM) could achieve an inhibition rate of 98% (Fig. 5*A*). In contrast, much higher concentrations of the other chemotherapeutic agents were required to achieve an 80–90% inhibition: (a) 360 ng/ml Adriamycin (663 nM); (b) 2700 ng/ml mitomycin (8.1 μM); and (c) 2490 ng/ml cisplatin (8.3 μM).

Similar effects were obtained with xenografts of MGC80-3 cells growing in nude mice. When such mice were treated with TPL at 0.15 mg/kg daily (i.p.), the tumor size was reduced by 90%, whereas those that were treated with Adriamycin (1.2 mg/kg), mitomycin (1.7 mg/kg), and cisplatin (7 mg/kg) weekly showed a reduction of 75–80%, which was less than the TPL group (Fig. 5*B*). These results demonstrated that the antitumor effect of TPL was comparable with or even superior to the three conventional chemotherapeutic drugs tested.
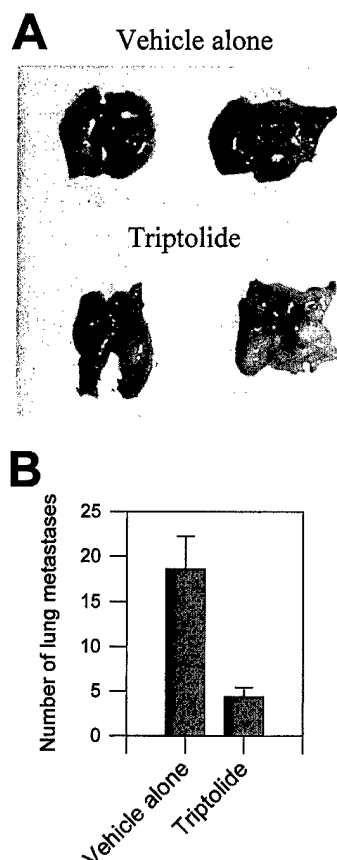
Fig. 4. Effect of TPL on experimental metastasis. B16F10 cells were injected into the tail veins of mice, and beginning 3 days later, TPL (0.15 mg/kg/day) and control vehicle were administered daily to the mice by i.p. injection. Two weeks later, the mice were sacrificed, and the lungs were dissected free. In *A*, representative lungs show that B16F10 metastases were reduced in mice receiving TPL as compared with vehicle controls. In *B*, the number of lung metastases was counted under a dissecting microscope in a double blind setting and indicated a significant difference between the TPL and control mice ($P < 0.01$). The experiment was repeated three times with similar results.

Fig. 5. Comparison of TPL with other chemotherapeutic drugs. In *A*, to compare the drugs *in vitro*, MGC80-3 cells were treated with: (a) vehicle alone (control); (b) TPL (10 ng/ml, 28 nM); (c) Adriamycin (360 ng/ml, 663 nM); (d) mitomycin (2700 ng/ml, 8.1 μM); and (e) cisplatin (2490 ng/ml, 8.3 μM). Two days later, the viability of the cells was determined by the MTT method. In *B*, to compare the drugs *in vivo*, mice with tumors 100 mm³ in size were divided into five groups and treated as follows: (a) vehicle alone (PBS); (b) TPL (0.25 mg/kg daily); (c) Adriamycin (1.2 mg/kg weekly); (d) mitomycin (1.7 mg/kg weekly); and (e) cisplatin (7 mg/kg weekly). Three weeks later, the mice were sacrificed, and the tumors were dissected and weighed. The data are expressed as inhibition % = (1 − mean of tumor weights of tests/mean of tumor weights of controls) × 100%.

Effect of TPL on Cells that Overexpress MDR1. One of the major problems encountered during the treatment of tumors with chemotherapeutic agents is the emergence of resistance caused by the expression of pumps on the plasma membrane of the tumor cells that remove drugs from the cytoplasm (17). In this experiment, we wanted to determine whether the effects of TPL were influenced by the expression of the MDR1 protein. To test this possibility, we examined a pair of MDA-435 cell lines that had been transduced with either a control retrovirus vector or one containing the MDR1 gene. As shown in Fig. 6*A*, although the control MDA-435 cells responded to Taxol at 10 ng/ml, this concentration of Taxol did not significantly affect the proliferation of the MDR1-overexpressing cells. However, these drug-resistant cells did show a significant response to TPL at 2 ng/ml. Similarly, TPL also inhibited the ability of MDR1-overexpressing cells to form colonies in soft agar (data not shown) and grow as tumor xenografts in nude mice (Fig. 6*B*). Thus, both *in vitro* and *in vivo* data strongly suggest that the TPL can circumvent the drug-resistant effects of MDR1.

Effect of TPL on Apoptosis and Cell Cycle Proteins. Because TPL inhibits the proliferation of tumor cells, we examined its effects on the induction of apoptosis. As shown in Fig. 7*A*, treatment of MDA-435 cells with TPL resulted in DNA fragmentation, the most definitive evidence that apoptosis is taking place. Next, we tested for molecules that control apoptosis and the cell cycle. The results of Western blotting revealed that TPL activated two key molecules in the apoptosis pathway, namely caspase 3 and PARP (Fig. 7, *B* and *C*). When MDA-435 cells were treated with TPL, there was an increase in the cleaved caspase 3 within 2 days and a shift in PARP from its intact molecule to a subunit (DNA catalytic domain) of M_r 89,000, which peaked on day 4 of treatment. The level of the M_r 89,000 PARP was greater in the TPL-treated group than in the Taxol-treated group, indicating that the antitumor action of TPL was different from the antimicrotubule Taxol. Western blotting analysis also revealed that the treatment with TPL for 3 days caused a significant reduction in c-*myc* and two pairs of cell cycle-promoting protein complexes, cyclin A/cdk2 and cyclin B/cdc2, and
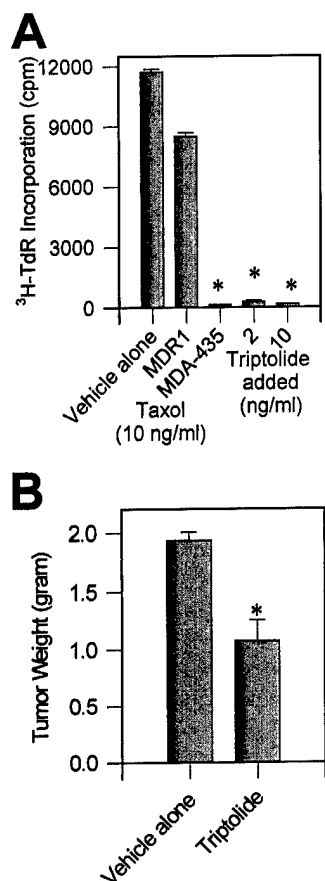
Fig. 6. Effect of TPL on cells that express the MDR1. A pair of MDA-435 cells that had been transfected with either a control retrovirus vector or one containing the MDR1 were tested for their sensitivities to TPL. In A, TPL inhibited the proliferation of MDA-435 cells that express the MDR1 gene as measured by [^{3}H]thymidine incorporation. However, these same cells were relatively resistant to Taxol. Similar results were obtained in a colony formation assay. In B, TPL (0.15 mg/kg/day) also inhibited the growth of MDR1 expressing MDA-435 cells in nude mice (see Fig. 3 for methods). Similar results were obtained in two replications.

cyclin D1 as well as the phosphorylated nonfunctional pRb (Fig. 7D). The inhibition of the cell cycle and induction of apoptosis may be responsible for antitumor effects of TPL.

Discussion

In this study, we have found that TPL has a number of attractive features as an antitumor agent. First, TPL appears to be active against a broad spectrum of tumors. In the mouse tumor model system, we found that the administration of TPL resulted in a 50–90% inhibition of primary tumors derived from the breast, bladder, stomach, and melanomas. In addition, other studies have shown that purified preparations of TPL were effective against cholangiocarcinomas in hamsters (11) and human breast cancer cells growing as xenografts in nude mice (10). Furthermore, TPL also blocked the formation of metastases in experimental mouse models involving the injection of B16 melanoma cells. Thus, TPL can inhibit the growth of both primary and secondary tumors.

A second feature of TPL is that in vivo, it appears to inhibit the growth of tumor cells regardless of their p53 status. We found that in mice, TPL inhibits the growth of tumor cells that possess both wild-type (B16) and mutated forms of p53 (MDA-435 and TSU; Refs. 22–24). This observation was somewhat surprising in view of several previous studies indicating that a functional p53 was required for the inhibitory effects of TPL on the growth of cultured tumor cells (9, 12), e.g., the suppression of p53 levels with antisense oligonucleotides has been reported to abrogate the induction of apoptosis by TPL in vitro (12). At present, the explanation for these conflicting results is unclear. Perhaps the in vitro results do not apply to the in vivo situation, which is far more complex and involves multiple factors, such as vascularization and the immune response. Regardless of the cause, the fact that TPL acts independently of p53 in vivo is advantageous, because a high proportion of tumors has p53 mutations or deletions and will still be targeted by TPL.

A third feature of TPL is that its antitumor activity is not adversely effected by the expression of the MDR1 protein, which inhibits the effects of other chemotherapeutic drugs. MDR1 is a transmembrane protein that is able to pump hydrophobic drugs out of the cytosol using an ATP-dependent mechanism. When we tested cells that had been induced to express high levels of MDR1 by an expression vector, these cells were still sensitive to the killing effects of TPL, although they were relatively resistant to the effects of Taxol, another commonly used chemotherapeutic agent. This feature is important because TPL will remain effective against tumors that have developed tolerance against other agents. In this regard, TPL should be considered for use against tumors that have developed tolerance or in combination with other chemotherapeutic drugs.

A fourth attractive feature of TPL is its high potency. When tested against tumor cells growing in tissue culture, TPL was much more effective on a molar basis than other chemotherapeutic agents, such as Taxol, Adriamycin, mitomycin, and cisplatin. Similarly, in the mouse model system, TPL was more potent than Adriamycin, mitomycin, or cisplatin in inhibiting the growth of tumor xenografts. The high potency of TPL greatly simplifies the administration of this drug.

However, TPL does have one major drawback as an antitumor agent, namely its toxicity. Shamon et al. (10) have reported that TPL had a modest antitumor effect on breast cancer cells when administered i.p. at a dose of 25 μg/mouse three times per week. However, when the dose was increased to 50 μg/mouse, it was lethal. In our hand, the therapeutic window (the ratio of lethal dose to effective dose) for TPL was about 4 (data not shown) or about twice as high as that reported by Shamon et al. This difference in therapeutic window between our results and that of Shamon et al. could be attributable to the different regimens that were used for the administration of the TPL. We injected a lower dose of TPL on a daily basis, whereas Shamon et al. used a higher dose three times per week.

Our studies have also suggested that TPL affects a number of pathways within the cell that could be responsible for its antitumor activity. First, TPL can induce apoptosis in cultured cells as indicated by DNA fragmentation, and in-
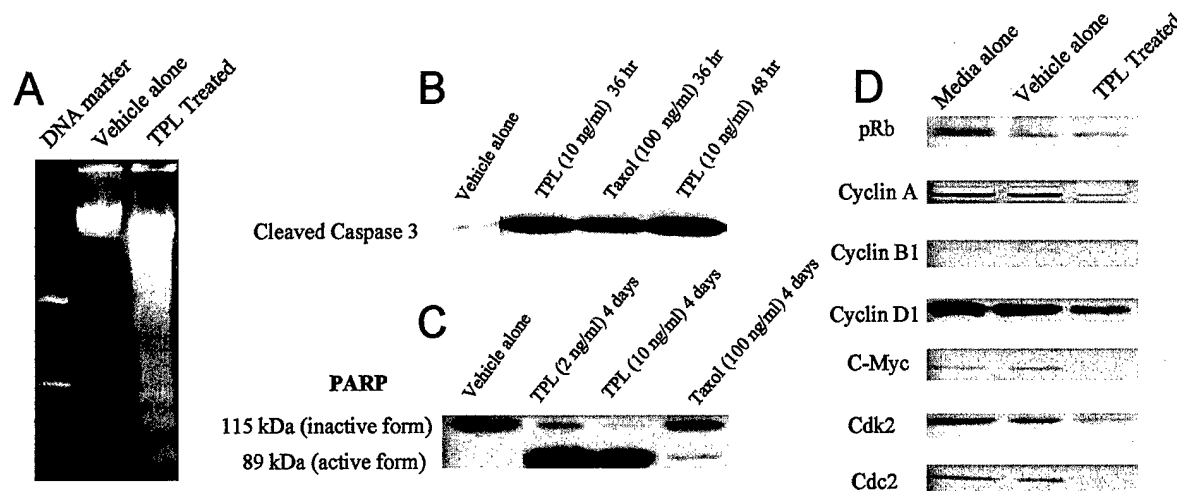
Fig. 7. Effect of TPL on apoptosis and cell regulatory molecules. Cultures of tumor cells at 80% confluence were incubated in the presence or absence of TPL (2 or 10 ng/ml) for different lengths of times, harvested, lysed, and analyzed for molecules related to apoptosis and cell cycle. In *A*, TSU cells treated with 10 ng/ml TPL for 3 days show laddering of the DNA indicative of apoptosis. In *B* and *C*, Western blotting of MDA-435 cells with antibodies specific for cleaved caspase 3 and to PARP show that these proteins were up-regulated by treatment with TPL. In *D*, Western blotting of MDA-435 cells shows that TPL treatments caused a reduction in the levels of phosphorylated (nonfunctional) pRb, cyclin A, cyclin B1, cyclin D1, c-*myc*, cdk2, and cdc2.

creased levels of caspase 3 and the cleaved form of PARP, all of which are markers of apoptosis. These results are consistent with other studies on cultured cells (9, 11, 12). At present, this appears to be the most likely mechanism by which TPL is able to block tumor growth. Although the TPL is probably acting directly on the tumor cells, it is possible that TPL also acts on the endothelial cells that are responsible for tumor vascularization as has been shown to be the case with other chemotherapeutic agents. Secondly, TPL reduces the levels of cell cycle-promoting factors, such as cyclin A/cdk2, cyclin B/cdc2, cyclin D1, and c-*myc*, as well as the phosphorylated (nonfunctional) form of pRb. These results are in keeping with those of Jiang *et al.* (12) who have shown that TPL arrests cells in the G_0-G_1 phase of the cycle. However, it is difficult to ascertain from this the upstream target of TPL because the reduction in these cell cycle regulators could result in cell apoptosis, and conversely, the apoptosis could reduce the synthesis of cell cycle-promoting factors.

Although TPL is known to activate a number of pathways within the cell, its specific upstream target remains unclear. Indeed, it is possible that TPL may target multiple molecules critical to cell survival. These molecules may, in turn, activate the various pathways that lead to suppression of the cell cycle and induction of apoptosis that inhibits the growth of primary and metastatic tumors. Clearly, future research should be directed toward the identification of the upstream molecules that are directly influenced by TPL.

In conclusion, TPL has very attractive features as an antitumor agent with regard to its broad spectrum of activity and potency. Potentially, TPL could be developed into a new antitumor agent.

References

1. Kupchan, S. M., Court, W. A., Dailey, R. G., Jr., Gilmore, C. J., and Bryan, R. F. Triptolide and tripdiolide, novel antileukemic ditepenoid tri-

poxides from Triterygium wilfordii. J. Am. Chem. Soc., *94:* 7194–7195, 1972.

2. Chen, B. J. Triptolide, a novel immunosuppressive and anti-inflammatory agent purified from a Chinese herb Tripterygium wilfordii Hook F. Leuk. Lymphoma, *42:* 253–265, 2001.

3. Chan, M. A., Kohlmeier, J. E., Branden, M., Jung, M., and Benedict, S. H. Triptolide is more effective in preventing T cell proliferation and interferon-gamma production than is FK506. Phytother. Res., *13:* 464–467, 1999.

4. Yang, Y., Liu, Z., Tolosa, E., Yang, J., and Li, L. Triptolide induces apoptotic death of T lymphocyte. Immunopharmacology, *40:* 139–149, 1998.

5. Huynh, P. N., Hikim, A. P., Wang, C., Stefonovic, K., Lue, Y. H., Leung, A., Atienza, V., Baravarian, S., Reutrakul, V., Swerdloff, R. S. Long-term effects of triptolide on spermatogenesis, epididymal sperm function, and fertility in male rats. J. Androl., *21:* 689–699, 2000.

6. Hikim, A. P., Lue, Y. H., Wang, C., Reutrakul, V., Sangsuwan, R., and Swerdloff, R. S. Posttesticular antifertility action of triptolide in the male rat: evidence for severe impairment of cauda epididymal sperm ultrastructure. J. Androl., *21:* 431–437, 2000.

7. Tao, X., Schulze-Koops, H., Ma, L., Cai, J., Mao, Y., and Lipsky, P. E. Effects of Tripterygium wilfordii Hook F extracts on induction of cyclooxygenase 2 activity and prostaglandin E2 production. Arthritis Rheum., *41:* 130–138, 1998.

8. Zhen, Q. S., Ye, X., and Wei, Z. J. Recent progress in research on Tripterygium: a male antifertity plant. Contraception, *51:* 120–129, 1995.

9. Chang, W. T., Kang, J. J., Lee, K. Y., Wei, K., Anderson, E., Gotmare, S., Ross, J. A., and Rosen, G. D. TPL and chemotherapy cooperate in tumor cell apoptosis: a role for the p53 pathway. J. Biol. Chem., *276:* 2221–2227, 2001.

10. Shamon, L. A., Pezzuto, J. M., Graves, J. M., Mehta, R. R., Wang-charoentrakul, S., Sangsuwan, R., Chaichana, S., Tuchinda, P., Cleason, P., and Reutrakul, V. Evaluation of the mutagenic, cytotoxic, and antitumor potential of TPL, a highly oxygenated diterpene isolated from Tripterygium wilfordii. Cancer Lett., *112:* 113–117, 1997.

11. Tengchaisri, T., Chawengkirttikul, R., Rachaphaew, N., Reutrakul, V., Sangsuwan, R., and Sirisinha, S. Antitumor activity of TPL against cholangiocarcinoma growth in vitro and in hamsters. Cancer Lett., *133:* 169–175, 1998.

12. Jiang, X. H., Wong, B. C., Lin, M. C., Zhu, G. H., Kung, H. F., Jiang, S. H., Yang, D., and Lam, S. K. Functional p53 is required for triptolide-

induced apoptosis and AP-1 and nuclear factor-kappa B activation in gastric cancer cells. Oncogene, 20: 8009–8018, 2001.

13. Lu, L. H., Lian, Y. Y., He, G. Y., Lin, S. P., Huan, S. H., Chen, Z. Z., Dend, H. X., and Zheng, Y. L. Clinical study of triptolide in treatment of acute leukemia. Clin. Exp. Investig. Hematol., 3: 1–3, 1992.

14. Li, K., Yuan, Y., Dai, X., and Qao, X. Determination of triptolide in extract from leigongteng (Tripterygium Wilfordii Hook. F.) by RP-HPLC. Se Pu, 16: 356–357, 1998.

15. Mao, Y. P., Tao, X. L., and Lipsky, P. E. Analysis of the stability and degradation products of triptolide. J. Pharm. Pharmacol., 52: 3–12, 2000.

16. Inove, S. Comparative study of concentrations of antitumor reagents in serum and tumor in nude mouse and human. In: B-Q. Wu and J. Zheng (eds.), Immune-deficient Animals in Experimental Medicine, pp. 323–325. 6th Int. Workshop on Immune-deficient Animals. Beijing, 1988; Basel: S. Karger AG, 1989.

17. Leonessa, F., Green, D., Licht, T., Wright, A., Wingate-Legette, K., Lippman, J., Gottesman, M. M., and Clarke, R. MDA435/LCC6 and MDA435/LCC6MDR1: ascites models of human breast cancer. Br. J. Cancer, 73: 154–161, 1996.

18. Sellins, K. S., and Cohen, J. J. Gene induction by gamma-irradiation leads to DNA fragmentation in lymphocytes. J. Immnol., 139: 3199–3206, 1987.

19. Gu, W. Z., Chen, R., Brandwein, S., McAlpine, J., and Burres, N. Isolation, purification, and characterization of immunosuppressive com-

pounds from tripterygium: triptolide and tripdiolide. Int. J. Immunophar-macol., 17: 351–356, 1995.

20. Zhang, C. P., Lu, X. Y., Ma, P. C., Chen, Y., Zhang, Y. G., Yan, Z., Chen, G. F., Zheng, Q. T., He, C. H., and Yu, D. Q. Studies on diterpenoids from leaves of Tripterygium wilfordii. Yao Xue Xue Bao, 28: 110–115, 1993.

21. Zheng, J. Screening of active anti-inflammatory, immunosuppressive and antifertility components of Tripterygium wilfordii. III. A comparison of the antiinflammatory and immunosuppressive activities of 7 diterpene lactone epoxide compounds in vivo. Zhong Guo Yi Xue Ke Xue Yuan Xue Bao, 13: 391–397, 1991.

22. Lentini, A., Vidal-Vanaclocha, F., Facchiano, F., Caraglia, M., Abbruzzese, A., and Beninati, S. Theophylline administration markedly reduces hepatic and pulmonary implantation of B16–F10 melanoma cells in mice. Melanoma Res., 10: 435–443, 2000.

23. van Bokhoven, A., Varella-Garcia, M., Korch, C., Hessels, D., and Miller, G. J. Widely used prostate carcinoma cell lines share common origins. Prostate, 47: 36–51, 2001.

24. O'Connor, P. M., Jackman, J., Bae, I., Myers, T. G., Fan, S., Mutoh, M., Scudiero, D. A., Monks, A., Sausville, E. A., Weinstein, J. N., Friend, S., Fornace, A. J., and Kohn, K. W. Characterization of the p53 tumor suppressor pathway in cell lines o f the National Cancer Institute Anticancer Drug Screen and correlations with the growth-inhibitory potency of 123 anticancer agents. Cancer Res., 57: 4285–4300, 1997.